

The Decay Rate of Bound Pion to Bound Muon

by

Nuzhat Anjum

A thesis submitted in partial fulfillment of the requirements for the degree of

Master of Science

Department of Physics

University of Alberta

©Nuzhat Anjum, 2023

Abstract

The decay rate of exotic atoms is of great importance due to their short lifetimes, which presents a challenge when attempting to probe them. The study of pionic atoms can open up a new area of physics, and experiments such as the PiHe collaboration have found a new method of laser spectroscopy for pionic helium. [1].

The first part of this thesis provides a rigorous calculation of the atomic form factor, which involves evaluating an integration of a slowly convergent and oscillatory integrand. The main goal is to transform the integral into a summation which is easy to compute from the computational perspective. Using the plane wave expansion, the integral is separated into two separate integrals, which are radial and angular integrals. The integral involving the product of Bessel functions and associated Laguerre polynomials is used to calculate the radial integral. The angular integral is evaluated using the Wigner's $3-j$ symbol. An explicit analytical expression for the discrete-discrete transition form factor is presented, exactly in the way they are implemented in the program. Atomic form factor is an important factor in the calculation of decay rate and scattering amplitude.

The second part of the thesis investigates the decay rate of the pion bound in a Coulomb potential, which is an exotic atom. The bound pion in a hydrogen atom is formed when an electron of an ordinary hydrogen atom is replaced by a negative pion. We consider the bound pion decaying into a bound muon, producing muonic hydrogen and a muon antineutrino. Using the form factor calculation from the first part, we present the decay rate of the bound pion and the most probable final state of the muon. In the calculation of decay rate, we considered the non-relativistic wave function of the initial and final particles, since the velocity of pion in hydrogen is of the order of αc , where α is the fine structure constant.

Preface

This thesis is arranged as follows: In Chapter 2, we studied the atomic form factor for unequal masses. The atomic form factor calculation is inspired by the decay rate of bound pion decay into a bound muon. We have implemented the technique of [2] and introduced different masses for the initial and final particles and generalized direction of transferred momentum, which we will use in our calculation of bound pion decay. Chapter 3 has the free pion decay calculation. In Chapter 4, we have introduced field operators to calculate free pion decay and extended the field operators and states for the bound field. Using the bound field operators, we have calculated bound pion to bound muon decay. The final decay formula includes the modulus squared of the form factor from Chapter 2, which is then integrated over the neutrino angle.

Recent experimental findings on pionic atoms by the experimenters at the Paul Scherrer Institute (PSI) is one of the main motivation behind this work. The idea of this work belongs to Prof. Andrzej Czarnecki. The mathematical formalism of Chapter 2 is from a collaboration with Mohammad Rashid Taher. I have developed the Julia package for form factor calculation and compared it with the previous Fortran codes. For Chapter 4, Prof. Andrzej Czarnecki helped me with the calculation. With the value of form factor from Chapter 2, we have calculated the decay rate of bound pion into bound muon decay.

Acknowledgments

First and foremost, praises and thanks to the Almighty for his showers of blessings throughout my research work to complete the research successfully.

I would like to express my sincere gratitude to my supervisor Prof. Andrzej Czarnecki for the continuous support of my M.Sc study and research, for his patience, motivation, enthusiasm, and immense knowledge. His guidance helped me in all the time of research and writing this thesis. Furthermore, I deeply appreciate his extensive support to equipping me with the research facilities.

Besides my supervisor, I would like to thank Dr. Wen Chan for his prompt help whenever I had questions during the first year of my study. Also, I thank Mason Protter for his generous advice on parallel computing with Julia.

I thank my fellow group members Mohammad Mubasher, Syed Navid, Rishap Lamichhane, and Monica Figueroa for making my university life more manageable and enjoyable with various discussions on life, physics, culture, and many more.

I am extremely grateful to my parents for their love, prayers, caring, and sacrifices for educating and preparing me for my future. My deepest gratitude is to my caring and supportive husband, Mohammad Rashid Taher. Your encouragement when the times got rough is much appreciated and duly noted. I would like to thank my younger brother, who always encourage me for my higher study. I also would like to thank my in laws for being unconventionally supportive.

Contents

1	Introduction	1
2	An Implementation of Atomic Form Factor for Non-equal Masses	4
2.1	Introduction	4
2.2	Analytical Expression for the Discrete-discrete Form Factors	5
2.3	Description of Programs	10
2.4	Test Run, Input and Output	10
2.5	Comparison with Previously Published Results	11
2.5.1	Comparison with Results from [3]	11
2.5.2	Comparison with Recently Published Results from [4]	13
2.6	Real and Imaginary Part	13
2.7	Challenges in Numerical Computation of the Form Factor	14
2.8	Generalized Form Factor	15
2.8.1	The Angle Between Transferred Momentum and Radial Vector	16
2.9	Why Julia?	17
2.10	Conclusion	19
3	The Decay Rate of Free Pion	20
3.1	Introduction	20
3.2	Free Pion Decay	21
4	Bound Pion to Bound Muon Decay	24
4.1	Introduction	24
4.2	Free Pion to Free Muon decay	24
4.3	Bound Pion to Bound Muon	26
4.3.1	The Value of Transferred Momentum and Ratio of Bohr Radii	30
4.3.2	Most Probable Final State	30
4.4	PSI Experiment	31

Bibliography	34
A Form Factor Code	37
A.1 Mathematica Code for Integration	37
A.2 Mathematica Code for Summation	38
A.3 Break Down of Mathematica Summation Calculation	38
A.4 The Name, Purpose, Usage and Output of Example Run	38
A.5 Julia Code	42
A.6 Modified ffdiff.f file used for comparison	42
A.7 The main program	43
B The Hydrogen Atom	44
B.1 The Schrödinger Equation for Hydrogen Atom	44
B.2 The Klein-Gordon Equation for Hydrogen Atom	49
B.3 Dirac Equation for Hydrogen Atom: Ground State	57

List of Tables

2.1 Form factors for different combinations. 12

A.1 Absolute value of Form factors. 42

List of Figures

1.1	The oscillatory integrand.	2
2.1	3D plot of discrete-discrete form factor.	11
2.2	The integration of the real and the imaginary part.	14
2.3	The angle between the transferred momentum, \mathbf{q} and radial vector \mathbf{r}	16
2.4	Division of programming languages by data types.	17
2.5	The plot is for the computation time for different number of form factors using Julia and Fortran.	19
3.1	Quark structure of a negatively charged pion, consisting of a down quark and an up anti-quark.	20
3.2	Feynman diagram of free pion decay.	21
4.1	Feynman diagram for bound pion decay	27
4.2	The figure shows the 3D plot with the contour of transition decay width.	31
A.1	Description of Mathematica code to calculate numerical integration.	37
A.2	Mathematica code to calculate the form factor using the Eq. (2.31).	38
A.3	The error given by the Mathematica code A.2.	39

Chapter 1

Introduction

In 1935, Yukawa first predicted the existence of the pion theoretically, which was considered a mediator for strong force [5]. From 1939 to 1942, Indian physicists D. M. Bose and Bibha Choudhuri used photographic plates to study cosmic rays in the high-altitude mountain of Darjeeling and found long curved ionizing tracks distinguishable from the tracks of alpha particles and protons. They identified that the cosmic particle is about 200 times the mass of an electron [6, 7, 8]. Due to the shortage of higher sensitive experiments, they could not confirm that the ionizing curve was for meson. Later in 1947, British physicist C. F. Powell proved the existence of pion [9]. Pion is the lightest hadron and was used as a probe for the strong interaction. It is easy to produce as it is produced when protons hit a target.

Mesonic atoms were first made around 1947 and have been used in the experiments to understand the behavior of the particle in atoms [10]. Due to the long lifetime of pion compared to the electronic interactions, it is used as a probe. Pionic atoms are made when the electron is replaced by the negative pion. These types of atoms are not stable; the pion can be absorbed by the nucleus, destroying the atom, which is governed by strong interaction. The pion can also emit characteristic photons while changing the state through electromagnetic interaction, and the pion can decay via weak interaction and produce muon. The produced muon is usually in the free state, but it can also be bound. We will calculate the decay rate of the pion bound in hydrogen, which decays into a bound muon. In calculating the matrix element, one crucial part is the calculation of form factors.

Hans Bethe formulated the calculation of form factors where he considered an atom in the initial state characterized by quantum numbers n_1, l_1, m_1 , and it emits or absorbs a photon and goes into a new state characterized by new quantum numbers n_2, l_2, m_2 . According to [11], the hydrogen-like discrete-discrete atomic form factor is the Fourier transform of $\phi_{n_2 l_2 m_2}^*(\mathbf{r})\varphi_{n_1 l_1 m_1}(\mathbf{r})$ with respect to transferred momentum \mathbf{q} , where $\varphi_{n_1 l_1 m_1}(\mathbf{r})$ and

$\phi_{n_2 l_2 m_2}(\mathbf{r})$ are initial and final particle wave functions:

$$F_{n_1 l_1 m_1}^{n_2 l_2 m_2}(\mathbf{q}) = \int d\mathbf{r} \phi_{n_2 l_2 m_2}^*(\mathbf{r}) e^{i\mathbf{q}\cdot\mathbf{r}} \phi_{n_1 l_1 m_1}(\mathbf{r}). \quad (1.1)$$

The master calculations of the atomic form factors were performed by Bethe, who found a simple analytical formula [11]. However, the atom states were described by parabolic quantum numbers. Bethe's formulation is used in [12] to calculate the bound-bound transition cross section in hydrogen-like atoms using the initial and final particle in parabolic coordinates and quantization axis along the transferred momentum.

The integrand of Eq. (1.1) is oscillatory and irregular, as shown in Fig. 1.1. The integral

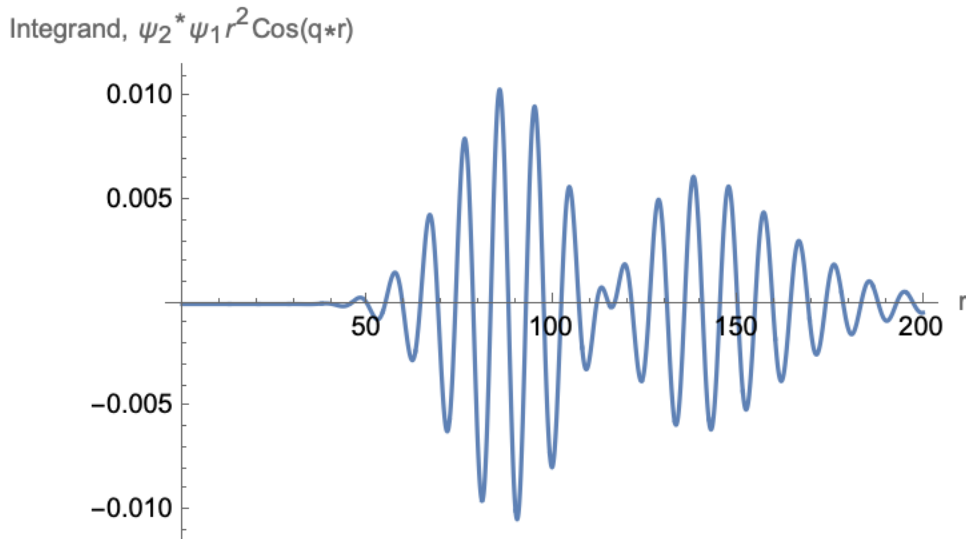


Figure 1.1: The integrand is not only oscillatory but also irregular, ψ_1 and ψ_2 with different Bohr radii multiplied with $\cos(qr)$ plotted as a function of r . The oscillatory integrand is very hard to evaluate numerically.

of Eq. (1.1) can be split into radial and angular integrals. The form factor calculation depends on the evaluation of the radial integral. The radial integral involves two associated Laguerre polynomials. The author of [3] used a Clebsch Gordan type linearization relation for the product of the two associated Laguerre polynomials. The integral containing Bessel functions is evaluated using the classical tables of integrals by Gradshteyn and Ryzhik [13] (entry 6.623.1), and the form factor is expressed in terms of Gegenbauer polynomials and used the quantization axis perpendicular to the transferred momentum. Another analytical formula for form factor was found by Massey and Mohr, which was also expressed in terms of Gegenbauer polynomials and used the atomic states in parabolic coordinates [14]. An alternative method of evaluating the radial integral is developed in [15] for dimuonium studies. The radial integral becomes the product of Bessel functions and the associated Laguerre

polynomials when one of the polynomials is expanded using the definition of Arfken and Weber [16]. This integral is evaluated using the mathematical result [17] and computed the diagonal atomic form factors for the quantization axis along transferred momentum. In this thesis, we have implemented this new technique of [15] to calculate the form factor for non-equal mass with an independent direction of transferred momentum. By the non-equal mass, we mean that the final particle mass changes through the decay or scattering processes.

A bound pion can be absorbed by the nucleus or decay through weak interaction, producing a muon (which can be bound or free) and a muon antineutrino. In this thesis, we consider the case where the final produced muon stays bound. To calculate the decay rate, we have used our formulated form factor calculation. In this decay process, we need the form factor for unequal masses since the initial and final particles are different.

Chapter 2

An Implementation of Atomic Form Factor for Non-equal Masses

2.1 Introduction

A form factor is an essential element in the calculation of the decay rate of bound particles. During decay, the particle changes into another particle or particles, and the mass is changed. Studying these types of decay requires the knowledge of form factors.

We have considered the technique of [2] and implemented different masses, introduced the independent direction of the quantization axis, and made a Julia package to calculate form factors.

Pionic hydrogen is an exotic atom. It is formed when an electron in the hydrogen atom is replaced by a pion. An exotic atom has a short lifetime because of the lifetime of the substitute particles. The lifetime of free π^- is $\tau_{\pi^-} = 26\text{ns}$. We can not assume that this lifetime resembles the lifetime of pionic hydrogen because the charged meson is bound.

Pionic hydrogen decays into muonic hydrogen. The Bohr radius of the pionic hydrogen and the muonic hydrogen is different because of their different masses. In the study of the bound pion decay rate, we need the discrete-discrete transition form factors for non-equal masses. A convenient formula for form factor for the equal mass was presented in [2]. In this chapter, we present a method for evaluating an integral, which is the Fourier transform of initial and final particle wave functions with respect to transferred momentum during decay.

2.2 Analytical Expression for the Discrete-discrete Form Factors

According to [11], the hydrogen-like discrete-discrete atomic form factor is the Fourier transform of $\phi_{n_2 l_2 m_2}^*(\mathbf{r})\phi_{n_1 l_1 m_1}(\mathbf{r})$ with respect to transferred momentum \mathbf{q} , where $\phi_{n_1 l_1 m_1}(\mathbf{r})$ and $\phi_{n_2 l_2 m_2}(\mathbf{r})$ are initial and final particle wave functions:

$$F_{n_1 l_1 m_1}^{n_2 l_2 m_2}(\mathbf{q}) = \int d\mathbf{r} \phi_{n_2 l_2 m_2}^*(\mathbf{r}) e^{i\mathbf{q}\cdot\mathbf{r}} \phi_{n_1 l_1 m_1}(\mathbf{r}) \quad (2.1)$$

$$= \int d\mathbf{r} R_{n_2 l_2}^*(r) Y_{l_2 m_2}(\Omega) e^{i\mathbf{q}\cdot\mathbf{r}} R_{n_1 l_1}(r) Y_{l_1 m_1}(\Omega), \quad (2.2)$$

where $Y_{lm}(\Omega)$ are spherical functions, $R_{nl}(r)$ is the hydrogen-like radial wave functions, and $d\mathbf{r} = r^2 dr d\Omega$, with $d\Omega = \sin\theta d\theta d\phi$. The radial wave functions of initial particle have the form

$$R_{n_1 l_1}(r) = \frac{2}{n_1^2} \sqrt{\frac{(n_1 - l_1 - 1)!}{(n_1 + l_1)!}} e^{-\frac{r}{n_1}} \left(\frac{2r}{n_1}\right)^{l_1} L_{n_1 - l_1 - 1}^{2l_1 + 1}\left(\frac{2r}{n_1}\right), \quad (2.3)$$

with L_n^m as the associated Laguerre polynomials. The associated Laguerre polynomials defined as in [16]

$$L_n^m(x) = (n + m)! \sum_{k=0}^n \frac{(-1)^k}{k!(n - k)!(k + m)!} x^k. \quad (2.4)$$

We are using the Bohr orbit of the initial particle, as the unit of length so the radial wave functions of the final particle can be written as

$$R_{n_2 l_2}(r) = \frac{2}{\rho^{3/2} n_2^2} \sqrt{\frac{(n_2 - l_2 - 1)!}{(n_2 + l_2)!}} e^{-\frac{r}{\rho n_2}} \left(\frac{2r}{\rho n_2}\right)^{l_2} L_{n_2 - l_2 - 1}^{2l_2 + 1}\left(\frac{2r}{\rho n_2}\right), \quad (2.5)$$

where $\rho = \frac{a_2}{a_1}$, with a_1 = initial particle Bohr radius and a_2 = final particle Bohr radius. We are implementing different masses through the ratio of Bohr radii.

It is possible to expand the plane wave given in eq. (2.2) as a sum over spherical harmonics

$$e^{i\mathbf{q}\cdot\mathbf{r}} = \sum_{l=0}^{\infty} \sum_{m=-l}^l j_l(qr) c_{lm}(\Omega_q) Y_{lm}^*(\Omega_r). \quad (2.6)$$

We can choose the direction of \mathbf{q} along z -axis. For $\mathbf{q} = q\hat{z}$, $\mathbf{q}\cdot\mathbf{r} = qr\cos\theta$, and θ is the polar angle between \mathbf{r} and the z -axis. Hence the double sum in eq. (2.6) must be independent of the azimuthal angle ϕ . This is possible only if $c_{lm}(q\hat{z}) = 0$ for all $m \neq 0$. That is, only the

$m = 0$ term of eq. (2.6) survives and it follows that

$$e^{iqr\cos\theta} = \sum_{l=0}^{\infty} \left(\frac{2l+1}{4\pi} \right)^{1/2} A_l(q) j_l(qr) P_l(\cos\theta), \quad (2.7)$$

where $A_l(q) \equiv c_{l0}(q\hat{z})$, and we have employed the relation between $Y_{l0}(\theta, \phi)$ and the Legendre polynomial, $P_l(\cos\theta)$. We can find the coefficient $A_l(q)$ by using the orthogonality relation of the Legendre polynomials. The coefficient is

$$A_l(q) = i^l \sqrt{4\pi(2l+1)}. \quad (2.8)$$

Using this coefficient in (2.7)

$$e^{iqr\cos\theta} = \sum_{l=0}^{\infty} i^l (2l+1) j_l(qr) P_l(\cos\theta) \quad (2.9)$$

Using the addition theorem of spherical harmonics,

$$P_l(\cos\theta) = \frac{4\pi}{2l+1} \sum_{m=-l}^l Y_{lm}(\mathbf{r}) Y_{lm}^*(\mathbf{q}), \quad (2.10)$$

the plane wave expansion becomes [18]

$$e^{i\mathbf{q}\cdot\mathbf{r}} = 4\pi \sum_{l=0}^{\infty} \sum_{m=-l}^l i^l j_l(qr) Y_{lm}(\Omega_q) Y_{lm}^*(\Omega_r), \quad (2.11)$$

Using this expansion in Eq. (2.2), we get

$$\begin{aligned} F_{n_1 l_1 m_1}^{n_2 l_2 m_2} &= 4\pi \sum_{l=0}^{\infty} \sum_{m=-l}^l \int_0^{\infty} r^2 dr R_{n_2 l_2}^*(r) R_{n_1 l_1}(r) i^l j_l(qr) \int Y_{lm}(\Omega_q) Y_{l_2 m_2}^*(\Omega_r) \\ &\quad \cdot Y_{l_1 m_1}^*(\Omega) Y_{l_1 m_1}(\Omega_r) d\Omega_r \end{aligned} \quad (2.12)$$

$$= 4\pi \sum_{l=0}^{\infty} \sum_{m=-l}^l \int_0^{\infty} r^2 dr R_{n_2 l_2}^*(r) R_{n_1 l_1}(r) i^l j_l(qr) Y_{lm}(\Omega_q) I_{l_1 l_2}^{m_1 m_2 m}, \quad (2.13)$$

where

$$I_{l_1 l_2 l}^{m_1 m_2 m} = \int d\Omega Y_{l_2 m_2}^*(\Omega) Y_{l m}^*(\Omega) Y_{l_1 m_1}(\Omega) \quad (2.14)$$

$$= (-1)^{m_2+m} \int d\Omega_r Y_{l_2, -m_2}(\Omega_r) Y_{l, -m}(\Omega_r) Y_{l_1 m_1}(\Omega_r). \quad (2.15)$$

The angular integral Eq. (2.15) can be expressed in terms of Wigner's 3j-symbol [19]

$$I_{l_1 l_2 l}^{m_1 m_2 m} = (-1)^{m_2+m} \sqrt{\frac{(2l_1+1)(2l_2+1)(2l+1)}{4\pi}} \begin{pmatrix} l_1 & l_2 & l \\ 0 & 0 & 0 \end{pmatrix} \cdot \begin{pmatrix} l_1 & l_2 & l \\ m_1 & -m_2 & -m \end{pmatrix} \quad (2.16)$$

$$= (-1)^{m_2+m} \sqrt{\frac{(2l_1+1)(2l_2+1)(2l+1)}{4\pi}} \mathcal{I}, \quad (2.17)$$

where $\mathcal{I} = \begin{pmatrix} l_1 & l_2 & l \\ 0 & 0 & 0 \end{pmatrix} \begin{pmatrix} l_1 & l_2 & l \\ m_1 & -m_2 & -m \end{pmatrix}$. The 3j-symbol $\begin{pmatrix} l_1 & l_2 & l \\ 0 & 0 & 0 \end{pmatrix}$ is nonzero only if $l + l_1 + l_2$ is an even integer [20], and $\begin{pmatrix} l_1 & l_2 & l \\ m_1 & -m_2 & -m \end{pmatrix}$ is nonzero only if $m = m_1 - m_2$ and $|l_1 - l_2| \leq l \leq l_1 + l_2$. So we can do the sum over l with a step of 2. We are using the Bohr orbit of the initial particle as the unit of length and initial particles reduced mass μ as the unit of mass. Introducing wave functions in the integral of Eq. (2.13) gives

$$F_{n_1 l_1 m_1}^{n_2 l_2 m_2} = 4\pi \frac{2^{2+l_1+l_2}}{(\rho)^{3/2} n_1^2 n_2^2} \sqrt{\frac{(n_1 - l_1 - 1)!}{(n_1 + l_1)!}} \sqrt{\frac{(n_2 - l_2 - 1)!}{(n_2 + l_2)!}} \sum_{l=|l_1-l_2|}^{l_1+l_2} \int_0^\infty r^2 dr e^{-\frac{r}{n_1}} \left(\frac{r}{n_1}\right)^{l_1} L_{n_1-l_1-1}^{2l_1+1} \left(\frac{2r}{n_1}\right) i^l j_l(qr) \cdot e^{-\frac{r}{\rho n_2}} \left(\frac{r}{\rho n_2}\right)^{l_2} L_{n_2-l_2-1}^{2l_2+1} \left(\frac{2r}{\rho n_2}\right) Y_{lm}(\Omega_q) I_{l_1 l_2 l}^{m_1 m_2 m}, \quad (2.18)$$

where $I_{l_1 l_2 l}^{m_1 m_2 m}$ is Eq. (2.16), and $\rho = \frac{a_2}{a_1}$.

$$F_{n_1 l_1 m_1}^{n_2 l_2 m_2} = N \sum_{l=|l_1-l_2|}^{l_1+l_2} i^l Y_{lm}(\Omega_q) I_{l_1 l_2 l}^{m_1 m_2 m} I_l, \quad (2.19)$$

where

$$N = \frac{4\pi 2^{2+l_1+l_2}}{\rho^{3/2+l_2} n_1^{2+l_1} n_2^{2+l_2}} \sqrt{\frac{(n_1 - l_1 - 1)!}{(n_1 + l_1)!}} \sqrt{\frac{(n_2 - l_2 - 1)!}{(n_2 + l_2)!}}, \quad (2.20)$$

$$I_l = \int_0^\infty r^{2+l_1+l_2} dr e^{-\frac{r}{n_1} - \frac{r}{\rho n_2}} L_{n_1-l_1-1}^{2l_1+1} \left(\frac{2r}{n_1} \right) j_l(qr) L_{n_2-l_2-1}^{2l_2+1} \left(\frac{2r}{\rho n_2} \right). \quad (2.21)$$

Now expanding $L_{n_2-l_2-1}^{2l_2+1}$ using Eqs. (2.4), and (2.21) becomes

$$I_l = \sum_{k=0}^{n_2-l_2-1} \frac{(-1)^k 2^k}{\rho^k n_2^k k! (n_2 - l_2 - 1 - k)! (2l_2 + k + 1)!} \cdot \int_0^\infty dr r^{2+l_1+l_2+k} e^{-\frac{rn_2\rho - rn_1}{\rho n_1 n_2}} L_{n_1-l_1-1}^{2l_1+1} \left(\frac{2r}{n_1} \right) j_l(qr). \quad (2.22)$$

Writing the spherical Bessel functions in terms of Bessel function of the first kind, and using the identity

$$j_n(x) = \sqrt{\frac{\pi}{2x}} J_{n+\frac{1}{2}}(x), \quad (2.23)$$

in Eq. (2.22), we get

$$I_l = \sqrt{\frac{\pi}{2q}} \sum_{k=0}^{n_2-l_2-1} \frac{(-1)^k 2^k}{\rho^k n_2^k k! (n_2 - l_2 - 1 - k)! (2l_2 + k + 1)!} \cdot \int_0^\infty dr r^{l_1+l_2+k+\frac{3}{2}} e^{-\frac{rn_2\rho - rn_1}{\rho n_1 n_2}} L_{n_1-l_1-1}^{2l_1+1} \left(\frac{2r}{n_1} \right) J_{l+\frac{1}{2}}(qr). \quad (2.24)$$

We can write

$$\gamma = l_1 + l_2 + k + \frac{3}{2}, \quad \delta = \frac{n_2\rho + n_1}{\rho n_1 n_2}, \quad \nu = l + \frac{1}{2}, \quad (2.25)$$

$$n = n_1 - l_1 - 1, \quad \beta = \frac{2}{n_1}, \quad \alpha = 2l_1 + 1, \quad (2.26)$$

and Eq. (2.24) becomes

$$I_l = \sqrt{\frac{\pi}{2q}} \sum_{k=0}^{n_2-l_2-1} \frac{(-1)^k 2^k}{\rho^k n_2^k k! (n_2 - l_2 - 1 - k)! (2l_2 + k + 1)!} \cdot \int_0^\infty e^{-\delta r} J_\nu(qr) r^\gamma L_n^\alpha(\beta r) dr. \quad (2.27)$$

The integration in Eq. (2.27) can be done using the following mathematical result [17]

$$\int_0^{\infty} e^{-\delta x} J_{\nu}(\mu x) x^{\gamma} L_n^{\alpha}(\beta x) dx = \sum_{k=0}^n \frac{(-\beta)^k \mu^{\nu} \Gamma(n + \alpha + 1) \Gamma(\nu + \gamma + k + 1)}{k! \Gamma(n - k + 1) \Gamma(\alpha + k + 1) 2^{\nu} \Gamma(\nu + 1) \delta^{\nu + \gamma + k + 1}} \cdot {}_2F_1\left(\frac{\nu + \gamma + k + 1}{2}, \frac{\nu + \gamma + k + 2}{2}; 1 + \nu; -\frac{\mu^2}{\delta^2}\right). \quad (2.28)$$

Using Eq. (2.28) in Eq. (2.27) gives

$$I_l = \sqrt{\frac{\pi}{2q}} \sum_{k=0}^{n_2 - l_2 - 1} \frac{(-1)^k 2^k}{\rho^k n_2^k k! (n_2 - l_2 - 1 - k)! (2l_2 + k + 1)!} \sum_{k_1=0}^n \frac{(-\beta)^{k_1} q^{\nu} \Gamma(n + \alpha + 1) \Gamma(\nu + \gamma + k_1 + 1)}{k_1! \Gamma(n - k_1 + 1) \Gamma(\alpha + k_1 + 1) 2^{\nu} \Gamma(\nu + 1) \delta^{\nu + \gamma + k_1 + 1}} \cdot {}_2F_1\left(\frac{\nu + \gamma + k_1 + 1}{2}, \frac{\nu + \gamma + k_1 + 2}{2}; 1 + \nu; -\frac{q^2}{\delta^2}\right). \quad (2.29)$$

Now introducing the expression for $Y_{lm}(\Omega_q)$

$$Y_{lm}(\Omega_q) = Y_{lm}(0, \phi) = \delta_{m0} \sqrt{\frac{2l + 1}{4\pi}}, \quad (2.30)$$

which corresponds to the case when the direction of the transferred momentum \mathbf{q} is taken as the direction of the quantization axis. The form factor is

$$F_{n_1 l_1 m_1}^{n_2 l_2 m_2} = N \sum_{l=|l_1 - l_2|}^{l_1 + l_2} A_l I_l, \quad (2.31)$$

where

$$A_l = i^l (-1)^{m_2 + m} \frac{2l + 1}{4\pi} \sqrt{(2l_1 + 1)(2l_2 + 1)} \mathcal{I}. \quad (2.32)$$

A similar result was obtained in Eq. (24) of [15]. The non-equal mass in this calculation comes through the Bohr radius. Because Bohr radius $\propto \frac{1}{\text{mass}}$. So, $\frac{a_2}{a_1} = \frac{\mu_1}{\mu_2}$, where μ_1 is the mass of the initial particle and μ_2 is the mass of the final particle. This formula (2.31) can be used in Python, Julia, Mathematica, or any other standard computer language. With $\rho = 1$, Eq. (2.31) reproduces all the results given in [21] for equal masses.

2.3 Description of Programs

We provide a Mathematica implementation of the discrete-discrete atomic form factor as given by Eq. (2.31).

- n_1 , l_1 , and m_1 are integers representing the quantum numbers of the initial atomic state.
- n_2 and l_2 are integers representing the quantum numbers of the final atomic state.
- ρ is floating point ratio of Bohr radii a_1 and a_2 . a_1 and a_2 are the Bohr radii of the initial and final particle respectively.
- q is the transferred momentum in atomic units. Atomic units: $q_{\text{atomic units}} = q/\mu$, where μ is the reduced mass of the hydrogen-like atom.

We have introduced another term called θ to implement the generalized direction of transferred momentum. The function is `mformq($n_1, l_1, m_1, n_2, l_2, m_2, \rho, q, \theta$)`.

- θ is the direction of transferred momentum and in radian units.

To make the formula easy to use so that one can calculate the form factor without knowing the source code; we developed a Julia package called `FormFactor`, which can be used as regular Julia packages. The Julia package and Mathematica code give the same result. The program is designed for Mac OS X and Windows 64bit and for Julia v1.7. The licensing of the program is MIT. We provide the Julia package for calculating the discrete-discrete atomic form factor. The Julia package can be used directly from the Github repository. To use this package, one has to run the following commands in Julia REPL

```
1 pkg> add https://github.com/nuzhat07/FormFactor.jl.git
2 julia> import FormFactor
3 julia> using FormFactor
4 julia> mform(1,0,0,1,0,1.0,0.66,0.0)
5 0.8132334486398062
```

2.4 Test Run, Input and Output

To illustrate the output of the program we plot the atomic form factors versus transferred momentum and the ratio of the Bohr radii. The following Fig. 2.1 is for $F_{4,2,0}^{5,0,0}(q)$, we can see that the discrete-discrete atomic form factor evaluated at zero transferred momentum is 0 because of the orthogonality of these states.

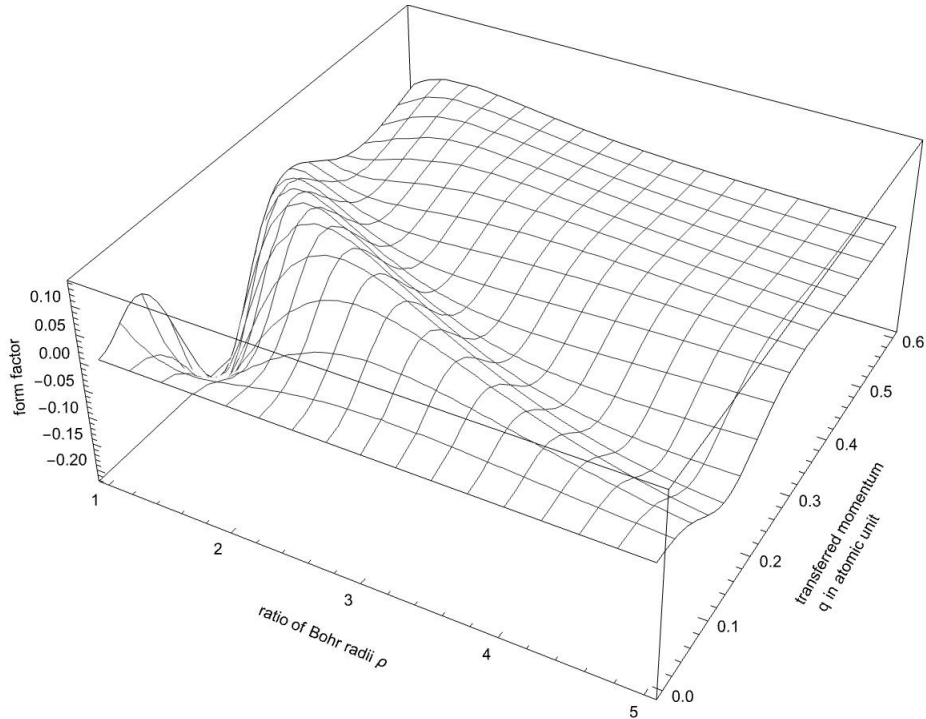


Figure 2.1: 3D plot of discrete-discrete form factor for transition from 4d to 5s versus transferred momentum and the ratio of the Bohr radii.

The output results and computation time for integration and summation are given in Table 2.1 for the following combinations of quantum numbers.

2.5 Comparison with Previously Published Results

2.5.1 Comparison with Results from [3]

Previously published literatures for form factor calculation only account for the equal masses. In our formula the mass comes through the value of the ratio of Bohr radii, ρ . So, for the comparison part, we inserted the value of ratio of Bohr radii, $\rho = 1$, which corresponds to the equal masses. The computation time of our Julia code for 30 form factors is 44.14s. We have compared the computation time with the previously published Fortran code [3] for the same quantum numbers. For the comparison, we have modified the “ffdiff.f” file given in A.6. We have changed the for loop in that file to calculate 30 form factors. The value of the transferred momentum and the combination of quantum numbers used in the Fortran code and in the Julia code were same. The computation time of the Fortran code is 4.88s. As expected the Julia code is almost 9 times slower than the Fortran code. The value of form

$n_1, l_1, m_1, n_2, l_2, \rho, q$	Form Factor (Integration)	Form Factor (Summation)	% deviation	Ratio of Integration Computation Time and Summation Computation Time
2, 1, 0, 1, 0, 0.5, 0.66	0.0883452 <i>i</i>	0.0883452 <i>i</i>	0	109892.0
3, 2, 0, 2, 1, 0.5, 0.66	0.0301999 <i>i</i>	0.0301999 <i>i</i>	0	53377.6
3, 1, 0, 2, 1, 0.5, 0.66	0.0587835	0.0587835	0	345396.0
3, 2, 1, 4, 2, 1.0, 0.66	-0.12248	-0.12247996	0	122265.0
4, 2, 2, 3, 2, 1.0, .66	0.0468502	0.04685025	0	111257.0
5, 3, 0, 4, 3, 0.5, 0.66	-0.0565619	-0.0565619	0	229612.0
5, 4, 3, 4, 3, 1.0, 0.66	0.00398216 <i>i</i>	0.00398216 <i>i</i>	0	130256.0
6, 4, 0, 2, 0, 0.5, 0.66	-0.00244159	-0.00244159	0	152241.0
9, 5, 0, 9, 5, 0.7, 0.66	-0.00783776	-0.00783776	0	314721.0
10, 9, 1, 9, 1, 1.0, .66	-0.00000066	-0.00000066	0	916695.0

Table 2.1: Form factors calculated using the integration and summation. The integration and summation using Eq. 2.31 are done in Mathematica. The function $F6$ in the appendix A.1 can calculate the integration. From comparing the computation time, we can say that our algorithm is almost 100000 times faster. Instead of doing the direct calculation of form factor, using this algorithm, we can save a lot of time and computation energy.

factor ranges between 0 to 1, our Julia code gives the value of form factor within the range up to $n = 40$.

2.5.2 Comparison with Recently Published Results from [4]

We are comparing the computation time with another recently published Fortran code [4]. But during the compilation of their Fortran code we have found an error which is published. The error is related to the `IMPLICIT NONE` statement. This statement is a non-executable statement. When it is used, the `IMPLICIT NONE` statement disables the typing provisions of Fortran. When the `IMPLICIT NONE` statement is included in a program, any variable that does not appear in an explicit type declaration statement is considered an error. While compiling we faced exactly the same error. In the published program file called `crsmumu.f`, inside three functions the `IMPLICIT NONE` statement was used by the authors but the type was not declared of the external functions. Through working with this, we have found the quick workaround. We can use a flag for the compiler which will ignore the out of date non-standard Fortran syntax. The flag is `-std=legacy`. We have written a main program using `DO` loop to calculate 30 form factors. We have used the functions written in the file `crsmumu.f`, taken the quantization axis along the transferred momentum, and chosen the computation method 1 which is [15]. The time to calculate 30 form factors is about 7s. If the output of a Fortran code has 3 digits in power we can use the format `ES11.2E3` to display the output.

2.6 Real and Imaginary Part

From our code it is visible that even values of l will contribute to the real form factor. If $l_1 + l_2 = \text{even}$ then l is always even since we are summing over l with a step of 2. On the other hand the form factor becomes imaginary for odd values of $l_1 + l_2$. For example the transition form factor F_{210}^{200} is imaginary because $l_1 + l_2 = 1$.

Also for the numerical integration, the imaginary and the real part of the integrand can be separated. Our integrand is

$$2\pi \iint r^2 dr \sin\theta d\theta \varphi_{n_2 l_2 m_2}^*(\mathbf{r}) e^{iqr \cos\theta} \varphi_{n_1 l_1 m_1}(\mathbf{r}) \quad (2.33)$$

which can be separated into two parts using Euler's formula. The integrand becomes

$$2\pi \iint r^2 dr \sin\theta d\theta \varphi_{n_2 l_2 m_2}^*(\mathbf{r}) (\cos(qr \cos\theta) + i \sin(qr \cos\theta)) \varphi_{n_1 l_1 m_1}(\mathbf{r}). \quad (2.34)$$

We can have different powers of r from the wave function. According to the definition of the

radial part of the wave function Eq.(2.3), r have powers of l . When the power of r is even we have only a real part in our numerical integration result. The sine function is odd and even power of r is even for this reason the numerical integration of the imaginary part vanishes. If $l_1 + l_2$ is even then r can have an even power. The imaginary part will survive when the power of r will be odd. If $l_1 + l_2$ is odd then r can have an odd power. This assumption can be checked by the result of two separate integration given below Fig. 2.2.

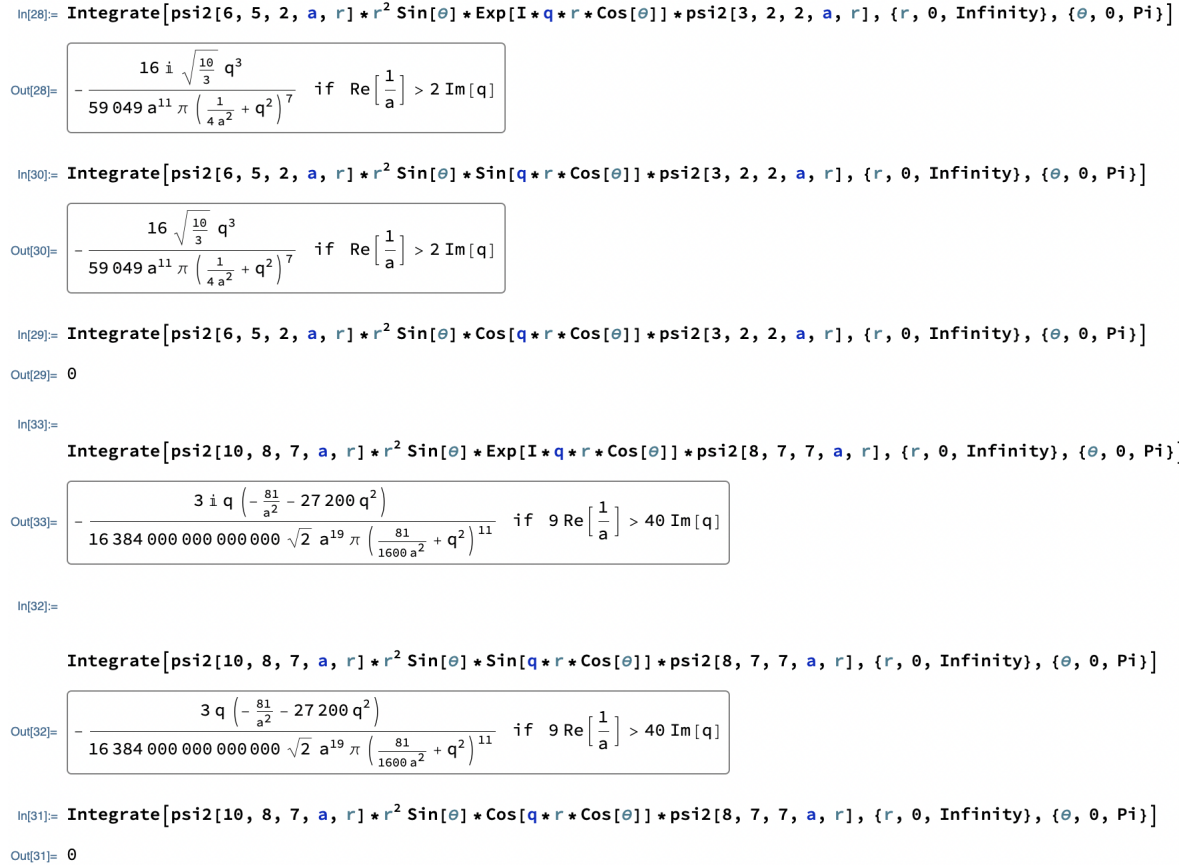


Figure 2.2: The integration is separated into two parts, one is real and another is imaginary part. The two results are compared.

2.7 Challenges in Numerical Computation of the Form Factor

The expression in Eq. (2.31) is adequate for the study of transitions between states of low and moderate values of principle quantum numbers about $n \approx 50$. This is because the expression gives rise to catastrophic cancellation errors or machine overflows for larger values of n , preventing the numerical work to progress [22]. The catastrophic cancellation

error is a numerical issue which arises when two numbers that are very close in value are subtracted from each other, resulting in a large error in final answer. The direct numerical computation of a hypergeometric function of large arguments depends on, in addition to the accuracy of the machine used, how skillfully the computer code is written. For high principle quantum number n the wave functions in the matrix element extends to a large distance from the nucleus. Also the ψ_{nlm} state with large n contains n^3 oscillations, arising from n nodes along each axis of the xyz coordinate system. Consequently, the matrix element got $n^3 \times n^3$ oscillations from wave functions and more oscillation can come from the operator. When a brute-force numerical technique is directly applied to evaluate the matrix element, these oscillations usually cause cancellation and/or rounding-off errors.

Also to avoid computation difficulty in Julia, we have replaced the factorials by Gamma functions since

$$\Gamma(n) = (n - 1)!, \quad (2.35)$$

where n is an integer.

The sum over l with a step of 2 reduces the memory allocation by 50% which increases the speed of the code.

In [3] they have mentioned that for $n = 13$, the deviation from the correct value is of the order of 1%. With our formula we can calculate the form factor which matches with the correct values from the integration up-to 8 decimal points. In [23], the author mentioned that Gordon formula shows problem after $n = 50$ and our formula shows problem after $n = 59$.

2.8 Generalized Form Factor

By generalized form factor, we mean that the direction of transferred momentum is independent of the z -axis. To get the generalized form factor, we have to get an independent z -axis other than the quantization axis. We can do that by using the generalized formula for the direction of the transferred momentum. We have to use general formula in Eq. (2.30) which is

$$Y_{lm}(\Omega_{\mathbf{q}}) = Y_{lm}(\theta, \phi) = (-1)^m \sqrt{\frac{(2l+1)\Gamma(l-m+1)}{4\pi\Gamma(l+m+1)}} P_l^m(\cos\theta) e^{im\phi}. \quad (2.36)$$

Here θ is the angle between the radial vector \mathbf{r} and transferred momentum \mathbf{q} , Fig.2.3.

2.8.1 The Angle Between Transferred Momentum and Radial Vector

Let us consider the angle between transferred momentum \mathbf{q} and the radial vector \mathbf{r} is θ . If we take the unit vectors in the direction of \mathbf{q} and \mathbf{r} respectively then we have

$$\hat{q} = \hat{x}\sin\theta_q\cos\phi_q + \hat{y}\sin\theta_q\sin\phi_q + \hat{z}\cos\theta_q, \quad (2.37)$$

$$\hat{r} = \hat{x}\sin\theta_r\cos\phi_r + \hat{y}\sin\theta_r\sin\phi_r + \hat{z}\cos\theta_r, \quad (2.38)$$

where θ_q and ϕ_q are the polar and azimuthal angle of \mathbf{q} and θ_r and ϕ_r are the polar and azimuthal angle of \mathbf{r} .

$$\begin{aligned} \cos\theta &= \hat{q} \cdot \hat{r} \\ &= \sin\theta_q\cos\phi_q\sin\theta_r\cos\phi_r + \\ &\quad \sin\theta_q\sin\phi_q\sin\theta_r\sin\phi_r + \cos\theta_q\cos\theta_r \\ &= \sin\theta_q\sin\theta_r\cos(\phi_r - \phi_q) + \cos\theta_q\cos\theta_r \end{aligned} \quad (2.39)$$

With the generalized direction of transferred momentum the form factor becomes

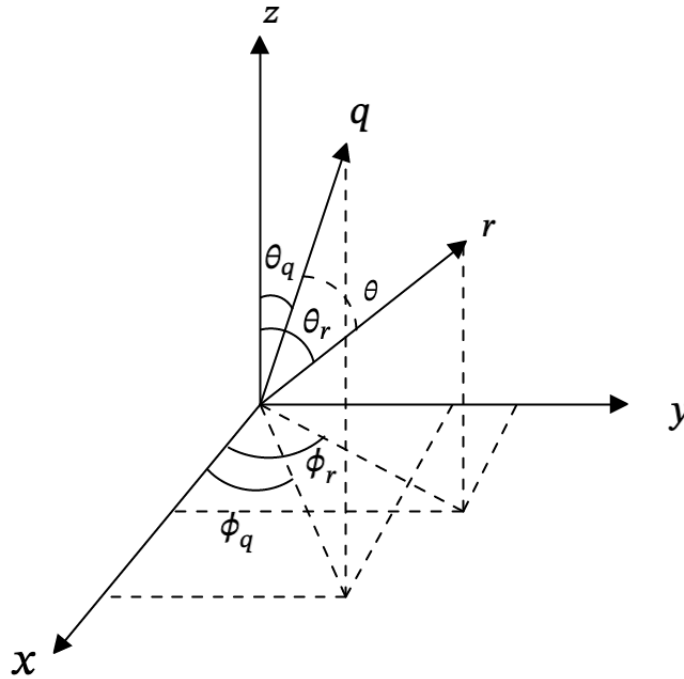


Figure 2.3: The angle between the transferred momentum, \mathbf{q} and radial vector \mathbf{r} .

$$F_{n_1 l_1 m_1}^{n_2 l_2 m_2} = N \sum_{l=|l_1-l_2|}^{l_1+l_2} B_l I_l, \quad (2.40)$$

where

$$B_l = i^l (-1)^{m_2+m} \sqrt{\frac{(2l_1+1)(2l_2+1)(2l+1)}{4\pi}} \mathcal{I}Y_{lm}(\theta_q, \phi_q), \quad (2.41)$$

and $Y_{lm}(\theta_q, \phi_q)$ is from Eq. (2.36)

2.9 Why Julia?

Julia, a very recent language, is developed by Jeff Bezanson, Stephan Karpinski, Viral B. Shah, and Alan Edelman in 2012 [24]. It is a high-level, Just In Time (JIT) compiled, a dynamic programming language for scientific, technical, and numerical computing [25]. Julia has the features of scripting language as well as the compiled language [25, 26]. There is a classification of programming language based on the appearance of the variable type. A programming language is statically typed if the type of a variable is known at compile time. On the other hand, a programming language is called dynamically typed if the type of a variable is a runtime object. Simply, dynamically typed language does not require defining the type of variables used in the program. That is why it is easy to write code in dynamic languages. User-friendly behavior comes at the cost of speed. Dynamic language takes more time during the runtime since it needs to check the type of variables in contrast to static language. Even though Julia is dynamically typed but it has a feature of user-defined type similar to static language.

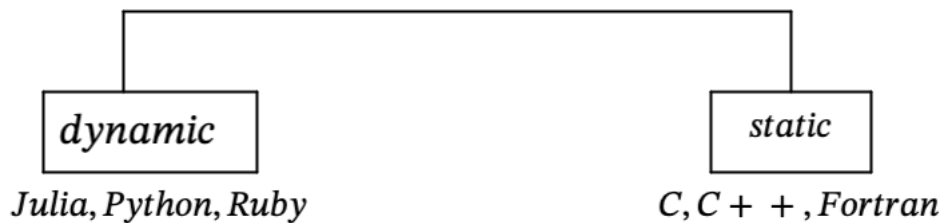


Figure 2.4: Division of programming languages by data types.

Another core virtue of Julia is JIT compilation with Low Level Virtual Machine (LLVM) compiler framework to generate machine code. LLVM defines an assembly-like language that Julia uses as a shared intermediate representation (IR) between different compiler optimization passes and other tools in the framework. There are three isomorphic forms of LLVM IR:

- A binary representation that is compact and machine readable.
- A textual representation that is verbose and somewhat human readable.
- An in-memory representation that is generated and consumed by LLVM libraries.

Julia uses LLVM's C++ API to construct LLVM IR in memory and then call some LLVM optimization passes on that form. LLVM compiler is also used by Fortran.

The first time we run a Julia function, it is parsed, and types are inferred. The JIT compiler then generates LLVM code, which is optimized and compiled down to native code. When the function is called a second time with arguments of a specific type, the already generated native code is called, resulting in much less time to run than the first time. The JIT compiler is a combination of Ahead Of Time (AOT) compilation and interpretation, converting the program source code into native machine code just before the program is run. This machine code is executed by the native hardware, which is more complex than the parsing and lowering to bytecode used by Python, but in exchange for the complexity, Julia gets its speed.

Python is also a dynamic language in contrast to Fortran or C, but why did we choose Julia over Python? Most dynamic languages are much slower than static languages. Python is an interpreted language that transforms the source code into bytecode, and the bytecode is then interpreted into machine code through a Python interpreter. Compiled languages are converted into machine code that the processor can execute. For this reason, Julia is faster than most other dynamic-interpreted languages.

Multiple dispatches, parallel computing, etc, make Julia unique. Using all of the arguments of the function to choose which method should be invoked, rather than just the first, is known as multiple dispatches [27]. Parallel computing can mean two things:

- Distributed computing: separate memory domains, using multiple cores on same machine or on different machines.
- Multi-threading: multiple cores on the same machine, all sharing memory.

Because of this multi-threading attribute, we were able to implement this in our code and got a better performance (see Fig. 2.5). We have introduced parallel computation in our code through the FLoops macro from Julia. FLoops is a macro that performs parallel iteration in Julia [28]. For this macro, our code works best with four threads in Julia, the Apple M1 processor, and 8 GB memory. We have plotted the computation time of the Julia one thread, Julia four thread, and Fortran code timing in Fig. 2.5. We can see that multi-threading reduces the computation time.

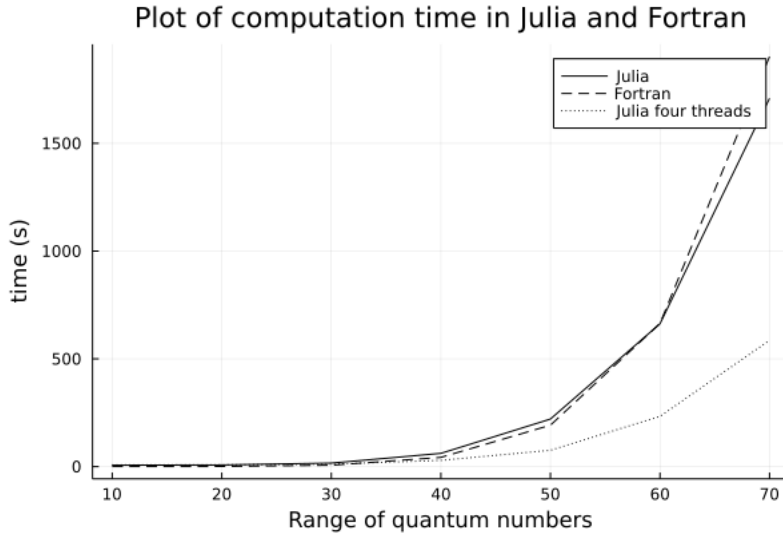


Figure 2.5: The plot is for the computation time for different number of form factors using Julia and Fortran. The compared Fortran form factor calculation is from [4]. For Julia, we have used single thread and multi-thread to do the computation. Multi-threading more efficient than single thread Julia and Fortran.

2.10 Conclusion

We have transformed the hard-to-evaluate integral Eq. (2.1) into a summation formula using the mathematical techniques described in the chapter. Using the summation formula, we have developed a package in Julia for the calculation of form factor, which can be used for any decay or scattering with a generalized direction of transferred momentum. The package takes only the input of the quantum numbers, the ratio of Bohr radii, the transferred momentum, and the direction of transferred momentum and gives the value of the form factor as an output. With our formula, one can calculate the form factor for a wider range of quantum numbers than in previous literature.

Chapter 3

The Decay Rate of Free Pion

3.1 Introduction

In 1935, Japanese physicist Yukawa Hideki predicted the existence of pion as the carrier particles of the strong force which was proven later in 1957 by British physicist Cecil F. Powell. Pion is considered as the hydrogen atom of quark model because it is simpler than a proton. Pion is made of a quark and an anti-quark. Pions are the lightest mesons with spin 0 and a mass of around 273 times of an electron. They are unstable, charged pion has a mean lifetime of 26ns. Pion usually decays into muon and muon anti neutrino $\pi^- \rightarrow \mu^- + \bar{\nu}_\mu$.

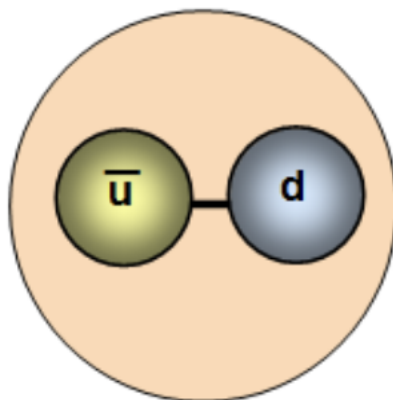


Figure 3.1: Quark structure of a negatively charged pion, consisting of a down quark and an up anti-quark.

3.2 Free Pion Decay

The decay rate of free pion calculation is inspired by an example from [29]. The decay of free charged pion (π^-) produces a muon (μ) and a muon antineutrino ($\bar{\nu}$). This process can be described by the Feynman diagram in Fig.3.2. The coupling of the pion with the W boson

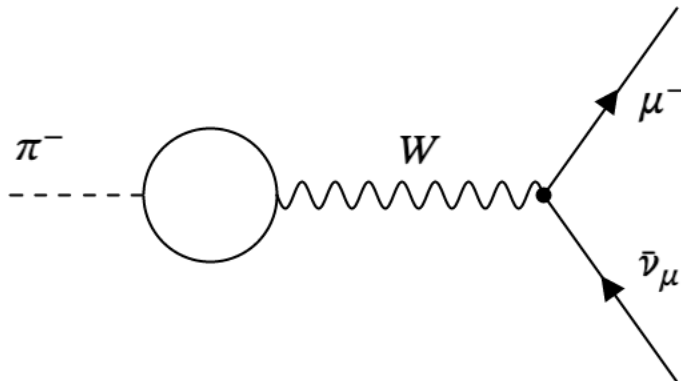


Figure 3.2: Feynman diagram of free pion decay. The decay happens via weak interaction producing muon and muon anti-neutrino. The blob is describing the coupling of π^- to W^- .

is defined by the blob in the figure. The golden rule for decay rate gives the decay width as [30]

$$\Gamma = \frac{1}{2m_\pi} \int d\Pi_{\text{LIPS}} |\mathcal{M}|^2 \quad (3.1)$$

Using the Feynman rules for amplitude, the matrix element becomes

$$\mathcal{M} = F^\alpha \cdot \left[\bar{u}(p_\mu) \frac{(-ig_w)}{2\sqrt{2}} \gamma^\alpha (1 - \gamma^5) v(p_{\bar{\nu}}) \frac{-ig_{\alpha\beta}}{M_w^2} \frac{-ig_w}{2\sqrt{2}} \right], \quad (3.2)$$

where g_w is the weak coupling constant, $g_w = \sqrt{4\pi\alpha_w}$, p_π , p_μ , $p_{\bar{\nu}}$ are the four momentum of pion, muon and anti neutrino respectively, M_w is the mass of the W^- boson and F^α is describing the $\pi^- \rightarrow W$ interaction. The $g_{\alpha\beta}$ from the propagator term contact with γ^α from the vertex factor and give the covariant γ_α . Dropping the overall i , we get

$$\mathcal{M} = \frac{g_w^2}{8M_w^2} [\bar{u}(p_\mu) \gamma_\alpha (1 - \gamma^5) v(p_{\bar{\nu}})] F^\alpha. \quad (3.3)$$

The F^α term should be a four vector to contract with γ_α . Since pion is a spin-less particle, the form factor can only be made with four momentum, $p_\pi = p$ of the pion. So the pion form

factor consists of a scalar quantity f_π times p^α

$$F^\alpha = f_\pi p^\alpha, \quad (3.4)$$

f_π is the pion decay constant. Squaring and summing over the outgoing spins, we get

$$|\mathcal{M}|^2 = \left[\frac{g_w^2 f_\pi}{8M_w^2} \right]^2 p^\alpha p^\beta [\bar{u}(p_\mu) \gamma_\alpha (1 - \gamma^5) v(p_{\bar{\nu}})] [\bar{u}(p_\mu) \gamma_\beta (1 - \gamma^5) v(p_{\bar{\nu}})]^*. \quad (3.5)$$

Using the Casimir trick [29],

$$\sum_{\text{all spins}} [\bar{u}(a) \Gamma_1 u(b)] [\bar{u}(a) \Gamma_2 u(b)]^* = \text{Tr} [\Gamma_1 (\not{p}_b + m_b) \bar{\Gamma}_2 (\not{p}_a + m_a)],$$

we can simplify the terms in the square brackets of Eq. 3.5 as

$$|\mathcal{M}|^2 = \left[\frac{g_w^2 f_\pi}{8M_w^2} \right]^2 p_\alpha p_\beta \text{Tr} [\gamma^\alpha (1 - \gamma^5) \not{p}_{\bar{\nu}} \gamma^\beta (1 - \gamma^5) (\not{p}_\mu + m_\mu)], \quad (3.6)$$

and after using the rules for trace calculation we have

$$|\mathcal{M}|^2 = \left[\frac{g_w^2 f_\pi}{8M_w^2} \right]^2 \cdot 8 [2(p \cdot p_{\bar{\nu}})(p \cdot p_\mu) - p^2(p_{\bar{\nu}} \cdot p_\mu)]. \quad (3.7)$$

Since $p = p_\mu + p_{\bar{\nu}}$ we can write

$$p \cdot p_{\bar{\nu}} = p_{\bar{\nu}} \cdot p_\mu, \quad p \cdot p_\mu = m_\mu^2 + p_{\bar{\nu}} \cdot p_\mu, \quad (3.8)$$

$$p^2 = p_{\bar{\nu}}^2 + p_\mu^2 + 2p_{\bar{\nu}} \cdot p_\mu, \quad 2p_{\bar{\nu}} \cdot p_\mu = (m_\pi^2 - m_\mu^2). \quad (3.9)$$

Thus the amplitude becomes

$$|\mathcal{M}|^2 = \left(\frac{g_w}{2M_w} \right)^4 f_\pi^2 m_\mu^2 (m_\pi^2 - m_\mu^2). \quad (3.10)$$

Now, we only need the integral of phase space

$$\begin{aligned}
\int d\Pi_{\text{LIPS}} &= \int \frac{(2\pi)^4 \delta^4(p_\pi - p_\mu - p_{\bar{\nu}})}{(2\pi)^3 2E_\mu (2\pi)^3 2E_{\bar{\nu}}} d^3\mathbf{p}_\mu d^3\mathbf{p}_{\bar{\nu}} \\
&= \int \frac{(2\pi)^4 \delta(m_\pi - p_\mu^0 - p_{\bar{\nu}}^0) \delta^3(\mathbf{p}_\mu + \mathbf{p}_{\bar{\nu}})}{(2\pi)^3 2E_\mu (2\pi)^3 2E_{\bar{\nu}}} d^3\mathbf{p}_\mu d^3\mathbf{p}_{\bar{\nu}} \\
&= \int \frac{2\pi \delta(m_\pi - p_\mu^0 - p_{\bar{\nu}}^0)}{(2\pi)^3 2E_\mu \cdot 2E_{\bar{\nu}}} d^3\mathbf{p}_{\bar{\nu}} \\
&= \int \frac{\delta(m_\pi - p_\mu^0 - p_{\bar{\nu}}^0)}{4\pi E_\mu E_{\bar{\nu}}} |\mathbf{p}_{\bar{\nu}}|^2 d^3\mathbf{p}_{\bar{\nu}} \\
&= \frac{1}{4\pi} \int \frac{\delta(m_\pi - u)}{u} |\mathbf{p}_{\bar{\nu}}| du \quad [u = p_\mu^0 + p_{\bar{\nu}}^0] \\
&= \frac{1}{4\pi} \frac{|\mathbf{p}_{\bar{\nu}}|}{m_\pi}, \tag{3.11}
\end{aligned}$$

The outgoing momenta for two body decay is

$$|\mathbf{p}_{\bar{\nu}}| = \frac{1}{2m_\pi} (m_\pi^2 - m_\mu^2), \tag{3.12}$$

and combining Eq. 3.11 and 3.12, phase space becomes

$$\int d\Pi_{\text{LIPS}} = \frac{1}{8\pi} \frac{m_\pi^2 - m_\mu^2}{m_\pi^2} \tag{3.13}$$

So

$$\Gamma = \frac{f_\pi^2}{256\pi m_\pi^3} \left(\frac{g_w}{M_w} \right)^4 m_\mu^2 (m_\pi^2 - m_\mu^2)^2. \tag{3.14}$$

With the following values [31]

$$m_\pi = 139.57 \times 10^6 \text{eV}, \quad M_w = 80.38 \times 10^9 \text{eV}, \quad f_\pi = 130.41 \times 10^6 \text{eV}, \tag{3.15}$$

$$m_\mu = 105.67 \times 10^6 \text{eV}, \quad g_w = 0.65, \tag{3.16}$$

life time, τ of free pion becomes

$$\tau = \frac{1}{\Gamma} = 26 \text{ns}. \tag{3.17}$$

The lifetime of free pion is a well known value.

Chapter 4

Bound Pion to Bound Muon Decay

4.1 Introduction

The exotic state of an atom is a state where the electron of an ordinary atom is replaced by other subatomic particles of the same charge. When the replacing subatomic particle is a meson, these exotic atoms are called mesonic. In 1947, theoretical studies by Enrico Fermi and Teller [32] concluded the existence of mesonic atoms. A Pionic hydrogen atom is an exotic atom because a negative pion replaces the electron of an ordinary atom to form it. In this chapter, first, we calculated the free pion decay into free muon using field-theoretic formalism. Then we used the field-theoretic approach again to calculate the bound pion to the bound muon decay by introducing states as a combination of plane waves.

4.2 Free Pion to Free Muon decay

Let us consider a free pion decay $\pi \rightarrow \mu\bar{\nu}$ caused by the interaction

$$\mathcal{H} = \pi\bar{\mu}\nu. \quad (4.1)$$

The scalar field is

$$\pi(x) = \int \frac{d^3p}{\sqrt{(2\pi)^3 2E_p}} (a_{\mathbf{p}}e^{-ipx} + \text{H.c.}), \quad [a_{\mathbf{p}}, a_{\mathbf{p}'}^\dagger] = \delta^3(\mathbf{p} - \mathbf{p}'). \quad (4.2)$$

The initial state is

$$|\pi_{\mathbf{p}}\rangle = \sqrt{(2\pi)^3 2E_p} a_{\mathbf{p}}^\dagger |0\rangle. \quad (4.3)$$

This choice of normalization is Lorentz-invariant,

$$\langle \pi_{\mathbf{p}} | \pi_{\mathbf{p}'} \rangle = 2E_p (2\pi)^3 \delta^3(\mathbf{p} - \mathbf{p}'). \quad (4.4)$$

This describes particles with density $2E_p$. Feynman [33] said, ‘‘This is a crazy normalization but very useful in practice. We shall always normalize in this way.’’

The spinor muon field is ([34], p. 430)

$$\mu(x) = \int \frac{d^3p}{\sqrt{(2\pi)^3 2E_p}} \sum_{r=1}^2 [b_{\mathbf{p}}^{(r)} u_{\mathbf{p}}^{(r)} e^{-ipx} + c_{\mathbf{p}}^{(r)\dagger} v_{\mathbf{p}}^{(r)} e^{ipx}], \quad (4.5)$$

$$\{b_{\mathbf{p}}^{(r)}, b_{\mathbf{p}'}^{(r')\dagger}\} = \delta^{rr'} \delta^3(\mathbf{p} - \mathbf{p}'), \quad u_{\mathbf{p}}^{(r)\dagger} u_{\mathbf{p}}^{(r)} = 2E_p. \quad (4.6)$$

The final-state muon with three-momentum $\boldsymbol{\mu}$ is described by

$$|\mu_{\boldsymbol{\mu}}\rangle = \sqrt{2E_{\boldsymbol{\mu}}} (2\pi)^3 b_{\boldsymbol{\mu}}^{(r)\dagger} |0\rangle, \quad (4.7)$$

$$\langle \mu_{\boldsymbol{\mu}} | \mu_{\boldsymbol{\mu}'} \rangle = 2E_{\boldsymbol{\mu}} (2\pi)^3 \delta^3(\mathbf{p} - \mathbf{p}'), \quad (4.8)$$

and analogously for the neutrino. The matrix element of \mathcal{H} is (suppressing spin indices), for the free-scalar decay,

$$\mathcal{T}_F = (2\pi)^4 \delta^4(p - \mu - \nu) \mathcal{M}_F = \langle \mu_{\boldsymbol{\mu}} \nu_{\boldsymbol{\nu}} | \mathcal{H} | \pi_{\mathbf{p}} \rangle \quad (4.9)$$

$$= 4G_F V_{ud} F_{\pi} p^{\alpha} \int d^4x \langle 0 | \sqrt{2E_{\boldsymbol{\mu}}} (2\pi)^3 b_{\boldsymbol{\mu}} \sqrt{2E_{\boldsymbol{\nu}}} (2\pi)^3 c_{\boldsymbol{\nu}} \quad (4.10)$$

$$\int \frac{d^3p}{\sqrt{(2\pi)^3 2E_p}} (a_{\mathbf{p}} e^{-ipx} + \text{H.c.}) \quad (4.11)$$

$$\int \frac{d^3q}{\sqrt{(2\pi)^3 2E_q}} (b_{\mathbf{q}}^{\dagger} u_{\mathbf{q}}^{\dagger} e^{-iqx} + c_{\mathbf{q}} v_{\mathbf{q}}^{\dagger} e^{-iqx}) \gamma^0 \gamma^{\alpha} \frac{1 - \gamma^5}{2} \quad (4.12)$$

$$\int \frac{d^3k}{\sqrt{(2\pi)^3 2E_k}} (b_{\mathbf{k}} u_{\mathbf{k}} e^{-ikx} + c_{\mathbf{k}}^{\dagger} v_{\mathbf{k}} e^{ikx}) \quad (4.13)$$

$$\sqrt{(2\pi)^3 2E_{\mathbf{p}'}} a_{\mathbf{p}'}^{\dagger} |0\rangle \quad (4.14)$$

$$= 4G_F V_{ud} F_{\pi} p^{\alpha} (2\pi)^4 \delta^4(p - \mu - \nu) [\bar{u}_{\boldsymbol{\mu}} \gamma^{\alpha} v_{\boldsymbol{\nu}R}], \quad (4.15)$$

where F_{π} is the pion decay constant, and V_{ud} is the relevant Cabibbo-Kobayashi-Maskawa (CKM) matrix element. Therefore the square of the matrix element summed over final state

muon spin is

$$|\bar{\mathcal{M}}_F|^2 = (4G_F V_{ud} F_\pi)^2 p^\alpha p^\beta \text{Tr} \left[(\not{p}_\mu + m_\mu) \gamma^\alpha \frac{1 - \gamma^5}{2} \not{p}_\nu \frac{1 + \gamma^5}{2} \gamma^\beta \right]. \quad (4.16)$$

The decay rate is

$$\Gamma(\pi \rightarrow \mu\nu) = \frac{(4G_F V_{ud} F_\pi)^2}{2m_\pi} p^\alpha p^\beta \text{Tr} \left[(\not{p}_\mu + m_\mu) \gamma^\alpha \frac{1 - \gamma^5}{2} \not{p}_\nu \frac{1 + \gamma^5}{2} \gamma^\beta \right] \quad (4.17)$$

$$\int \frac{d^3\mu}{(2\pi)^3} \frac{d^3\nu}{2E_\mu (2\pi)^3 2E_\nu} (2\pi)^4 \delta^4(p - \mu - \nu) \quad (4.18)$$

$$= \frac{(2G_F V_{ud} F_\pi)^2}{2m_\pi} p^\alpha p^\beta \text{Tr} \left[(\not{p}_\mu + m_\mu) \gamma^\alpha (1 - \gamma^5) \not{p}_\nu (1 + \gamma^5) \gamma^\beta \right] \quad (4.19)$$

$$\frac{1}{4\pi} \frac{|\mathbf{p}_\nu|}{m_\pi}. \quad (4.20)$$

The outgoing momenta for two body decay is

$$|\mathbf{p}_\nu| = \frac{1}{2m_\pi} (m_\pi^2 - m_\mu^2). \quad (4.21)$$

The decay rate becomes

$$\Gamma(\pi \rightarrow \mu\nu) = \frac{(2G_F V_{ud} F_\pi)^2}{2m_\pi} m_\mu^2 \frac{(m_\pi^2 - m_\mu^2)}{2} \quad (4.22)$$

$$\frac{1}{8\pi m_\pi^2} (m_\pi^2 - m_\mu^2). \quad (4.23)$$

$$= \frac{(G_F V_{ud} F_\pi)^2}{8\pi m_\pi^3} m_\mu^2 (m_\pi^2 - m_\mu^2)^2 \quad (4.24)$$

The last equation of this section Eq. (4.24) also gives the 26ns lifetime as it should be.

4.3 Bound Pion to Bound Muon

The interaction is bound pion decay into bound muon which is $Z\pi^- \rightarrow Z\mu^- + \bar{\nu}_\mu$, described by the Feynman diagram Fig. (4.1). The initial bound state of the pion $|i\rangle$ is a combination

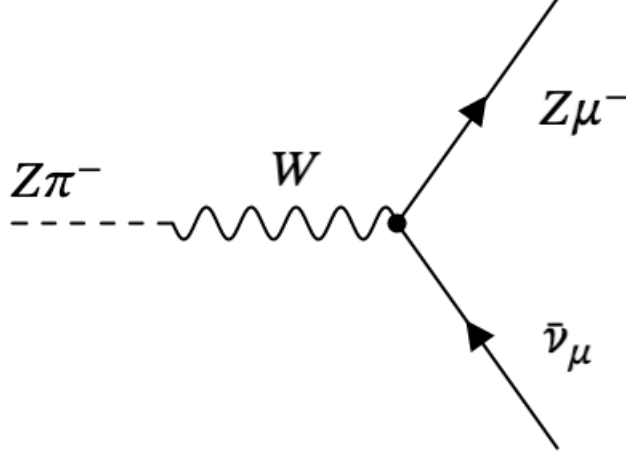


Figure 4.1: Feynman diagram for bound pion decay

of plane waves, instead of a single plane wave $|\phi_{\mathbf{p}}\rangle = \sqrt{(2\pi)^3} 2E_{\mathbf{p}} a_{\mathbf{p}}^{\dagger} |0\rangle$,

$$|i\rangle = \int \frac{d^3\mathbf{p}}{\sqrt{(2\pi)^3}} \varphi(\mathbf{p}) a_{\mathbf{p}}^{\dagger} |0\rangle, \quad (4.25)$$

$$1 = \langle i|i\rangle = \int \frac{d^3\mathbf{p}}{\sqrt{(2\pi)^3}} \varphi^*(\mathbf{p}) \frac{d^3\mathbf{q}}{\sqrt{(2\pi)^3}} \varphi(\mathbf{q}) \delta^3(\mathbf{p} - \mathbf{q}) \quad (4.26)$$

$$= \int \frac{d^3\mathbf{p}}{(2\pi)^3} |\varphi(\mathbf{p})|^2 = \int d^3\mathbf{r} |\psi(\mathbf{r})|^2. \quad (4.27)$$

Also, the final state muon is described by a combination of plane waves. Instead of $|\mu_{\mu}\rangle = \sqrt{2E_{\mu}} (2\pi)^3 b_{\mu}^{(r)\dagger} |0\rangle$, now

$$|\mu_B\rangle = \int \frac{d^3\mathbf{p}}{\sqrt{(2\pi)^3}} \varphi_{(\mu)}(\mathbf{p}) b_{\mathbf{p}}^{\dagger} |0\rangle, \quad (4.28)$$

analogously to Eq. (4.25), with $\int \frac{d^3\mathbf{p}}{(2\pi)^3} |\varphi_{(\mu)}(\mathbf{p})|^2 = 1$. And the final state neutrino is described by

$$|\nu\rangle = \sqrt{(2\pi)^3} 2E_{\nu} c_{\nu}^{\dagger} |0\rangle. \quad (4.29)$$

The scalar pion field is

$$\phi(x) = \int \frac{d^3p}{\sqrt{(2\pi)^3} 2E_p} (a_{\mathbf{p}} e^{-ipx} + \text{H.c.}), \quad [a_{\mathbf{p}}, a_{\mathbf{p}'}^{\dagger}] = \delta^3(\mathbf{p} - \mathbf{p}'). \quad (4.30)$$

The spinor muon field is ([34], p. 430)

$$\mu(x) = \int \frac{d^3p}{\sqrt{(2\pi)^3 2E_p}} \sum_{r=1}^2 [b_{\mathbf{p}}^{(r)} u_{\mathbf{p}}^{(r)} e^{-ipx} + c_{\mathbf{p}}^{(r)\dagger} v_{\mathbf{p}}^{(r)} e^{ipx}], \quad (4.31)$$

$$\{b_{\mathbf{p}}^{(r)}, b_{\mathbf{p}'}^{(r')\dagger}\} = \delta^{rr'} \delta^3(\mathbf{p} - \mathbf{p}'), \quad u_{\mathbf{p}}^{(r)\dagger} u_{\mathbf{p}}^{(r)} = 2E_p. \quad (4.32)$$

The bound-to-bound \mathcal{T} -matrix element is

$$\mathcal{T}_{BB} = \langle \mu_{\mu} \nu_{\nu} | \mathcal{H} | i \rangle \quad (4.33)$$

$$= 4G_{\text{F}} V_{\text{ud}} F_{\pi} p^{\alpha} \int d^4x \langle 0 | \sqrt{(2\pi)^3 2E_{\nu}} c_{\nu} \int \frac{d^3q'}{\sqrt{(2\pi)^3}} \varphi_{(\mu)}(\mathbf{q}') b_{\mathbf{q}'} \quad (4.34)$$

$$\int \frac{d^3p}{\sqrt{(2\pi)^3 2E_p}} (a_{\mathbf{p}} e^{-ipx} + \text{H.c.}) \quad (4.35)$$

$$\int \frac{d^3q}{\sqrt{(2\pi)^3 2E_q}} (b_{\mathbf{q}}^{\dagger} u_{\mathbf{q}}^{\dagger} e^{iqx} + c_{\mathbf{q}} v_{\mathbf{q}}^{\dagger} e^{-iqx}) \gamma^0 \gamma^{\alpha} \frac{1 - \gamma^5}{2} \quad (4.36)$$

$$\int \frac{d^3k}{\sqrt{(2\pi)^3 2E_k}} (b_{\mathbf{k}} u_{\mathbf{k}} e^{-ikx} + c_{\mathbf{k}}^{\dagger} v_{\mathbf{k}} e^{ikx}) \quad (4.37)$$

$$\int \frac{d^3\mathbf{p}'}{\sqrt{(2\pi)^3}} \varphi(\mathbf{p}') a_{\mathbf{p}'}^{\dagger} |0\rangle \quad (4.38)$$

$$= 4G_{\text{F}} V_{\text{ud}} F_{\pi} p^{\alpha} \int d^4x \int \frac{d^3q}{(2\pi)^3 \sqrt{2E_q}} \varphi_{(\mu)}(\mathbf{q}) \frac{d^3\mathbf{p}}{(2\pi)^3 \sqrt{2E_p}} \varphi(\mathbf{p}) \bar{u}_{\mathbf{q}} \gamma^{\alpha} v_{\nu R} e^{-i(p-q-\nu)x} \quad (4.39)$$

$$= \frac{4G_{\text{F}} V_{\text{ud}} F_{\pi} p^{\alpha} 2\pi \delta(m_{\pi} - m_{\mu} - E_{\nu})}{2\sqrt{m_{\pi} m_{\mu}}} \int d^3\mathbf{r} \int \frac{d^3q}{(2\pi)^3} \varphi_{(\mu)}(\mathbf{q}) \frac{d^3\mathbf{p}}{(2\pi)^3} \varphi(\mathbf{p}) \bar{u}_{\mathbf{q}} \gamma^{\alpha} v_{\nu R} e^{i(\mathbf{p}-\mathbf{q}-\nu)\cdot\mathbf{r}} \quad (4.40)$$

$$= \frac{2G_{\text{F}} V_{\text{ud}} F_{\pi} 2\pi \delta(m_{\pi} - m_{\mu} - E_{\nu})}{\sqrt{m_{\pi} m_{\mu}}} p^{\alpha} [\bar{u}_{\mathbf{q}} \gamma^{\alpha} v_{\nu R}] \int d^3\mathbf{r} \tilde{\varphi}_{(\mu)}^*(\mathbf{r}) \tilde{\varphi}_{(i)}(\mathbf{r}) e^{-i\nu\cdot\mathbf{r}}. \quad (4.41)$$

In this calculation, we used the non relativistic approximation for the scalar's and for the muon's energies, replacing them by masses. The spatial integral involving the muon and the scalar spatial wave functions and the plane wave factor representing the neutrino is the transition form factor from chapter (2); it is dimensionless. \mathcal{T}_{BB} has units of mass in power

$-2 + 1 - 1 - 1 + 1 + 1 = -1$. The rate is

$$\Gamma(\pi_B \rightarrow \mu_B \nu) = \sum_{\text{pol.}\mu,\nu} \frac{1}{T} \int \frac{d^3\nu}{(2\pi)^3 2E_\nu} |\mathcal{T}_{BB}|^2 \quad (4.42)$$

$$= \frac{1}{T} \int \frac{d^3\nu}{(2\pi)^3 2E_\nu} \frac{4\pi^2 T (2G_F V_{ud} F_\pi)^2 \delta(m_\pi - m_\mu - E_\nu)}{m_\pi m_\mu} p^\alpha p^\beta \text{Tr} [(\not{p}_\mu + m) \gamma^\alpha (1 - \gamma^5) \not{p}_\nu (1 + \gamma^5) \gamma^\beta] \left| \int d^3\mathbf{r} \tilde{\varphi}_{(\mu)}^*(\mathbf{r}) \tilde{\varphi}(\mathbf{r}) e^{-i\nu\cdot\mathbf{r}} \right|^2 \quad (4.43)$$

$$= \int \frac{d\Omega E_\nu dE_\nu}{4\pi} \frac{(2G_F V_{ud} F_\pi)^2 \delta(m_\pi - m_\mu - E_\nu)}{m_\pi m_\mu} m_\mu^2 \frac{(m_\pi^2 - m_\mu^2)}{2} \left| \int d^3\mathbf{r} \tilde{\varphi}_{(\mu)}^*(\mathbf{r}) \tilde{\varphi}(\mathbf{r}) e^{-i\nu\cdot\mathbf{r}} \right|^2 \quad (4.44)$$

$$= \frac{(m_\pi - m_\mu) (2G_F V_{ud} F_\pi)^2}{4\pi m_\pi m_\mu} m_\mu^2 \frac{(m_\pi^2 - m_\mu^2)}{2} \quad (4.45)$$

$$\int d\Omega \left| \int d^3\mathbf{r} \tilde{\varphi}_{(\mu)}^*(\mathbf{r}) \tilde{\varphi}(\mathbf{r}) e^{-i\nu\cdot\mathbf{r}} \right|^2 \quad (4.46)$$

$$= \frac{(m_\pi - m_\mu) (2G_F V_{ud} F_\pi)^2}{4\pi m_\pi m_\mu} m_\mu^2 \frac{(m_\pi^2 - m_\mu^2)}{2} \quad (4.47)$$

$$\int d\Omega \left| \int d^3\mathbf{r} \tilde{\varphi}_{(\mu)}^*(\mathbf{r}) \tilde{\varphi}(\mathbf{r}) e^{-i\nu\cdot\mathbf{r}} \right|^2 \quad (4.48)$$

$$= \frac{(m_\pi - m_\mu) (2G_F V_{ud} F_\pi)^2}{4\pi m_\pi m_\mu} m_\mu^2 \frac{(m_\pi^2 - m_\mu^2)}{2} \quad (4.49)$$

$$\int d\Omega \left| \int d^3\mathbf{r} \tilde{\varphi}_{(\mu)}^*(\mathbf{r}) \varphi_{(\pi)}(\mathbf{r}) e^{-i\nu\cdot\mathbf{r}} \right|^2. \quad (4.49)$$

It has units of mass in power $+1 + 3 - 1 + 2(-1) = 1$. We took the factor from trace out of the integral over neutrino angles because if the muon is taken at rest, this trace does not depend on neutrino direction.

Now, we can find the expression for the ratio of bound pion decay rate to the free pion decay rate, using Eq. (4.24) and Eq. (4.49)

$$\frac{\Gamma(\pi_B \rightarrow \mu_B \nu)}{\Gamma(\pi \rightarrow \mu \nu)} = \frac{4m_\pi^2 (m_\pi - m_\mu)}{m_\mu (m_\pi^2 - m_\mu^2)} \int d\Omega \left| \int d^3\mathbf{r} \tilde{\varphi}_{(\mu)}^*(\mathbf{r}) \varphi_{(\pi)}(\mathbf{r}) e^{-i\nu\cdot\mathbf{r}} \right|^2. \quad (4.50)$$

4.3.1 The Value of Transferred Momentum and Ratio of Bohr Radii for Pionic Hydrogen Decay

We are considering the pionic hydrogen is at rest and also the decay product muonic hydrogen is at rest and the transferred momentum is conveyed to muon anti neutrino. The transferred momentum is coming from the change of mass of the initial to final particle. With these information we can calculate the value of transferred momentum for this decay. The free pion and muon masses are respectively 139.57MeV and 105.7MeV. But the bound pionic and muonic hydrogen masses are the reduced mass of pionic and muonic hydrogen. The reduced mass formula is

$$\mu = \frac{m_1 m_2}{m_1 + m_2}. \quad (4.51)$$

So the reduced mass of pionic hydrogen is

$$\begin{aligned} \mu_\pi &= \frac{m_p m_\pi}{m_p + m_\pi} \\ &= \frac{938.27 \times 139.6}{938.27 + 139.6} \\ &= 121.52\text{MeV}. \end{aligned} \quad (4.52)$$

And the reduced mass of muonic hydrogen is

$$\mu_\mu = 94.99\text{MeV}. \quad (4.53)$$

The value of transferred momentum in atomic units would be

$$q = \frac{\mu_\pi - \mu_\mu}{\mu_\pi} = \frac{(139.57 - 105.7)}{139.57} = 0.24. \quad (4.54)$$

In our form factor formula, we have introduced the ratio of Bohr radii ρ in Chapter 2. Since the Bohr radius is inversely proportional to the mass of the respective particle. The numerical value of the ratio of Bohr radii would be

$$\rho = \frac{a_\mu}{a_\pi} = \frac{m_\pi}{m_\mu} = 1.28. \quad (4.55)$$

4.3.2 Most Probable Final State

If the pion is initially in $(n, l) = (17, 16)$ state and decays into muon, we can find the most probable final state. Since we can use our formula to write the decay width as a function of final state values. The 3D plot of n , l , and decay width will give a peak, which represents

the state with the highest decay width Fig. 4.2.

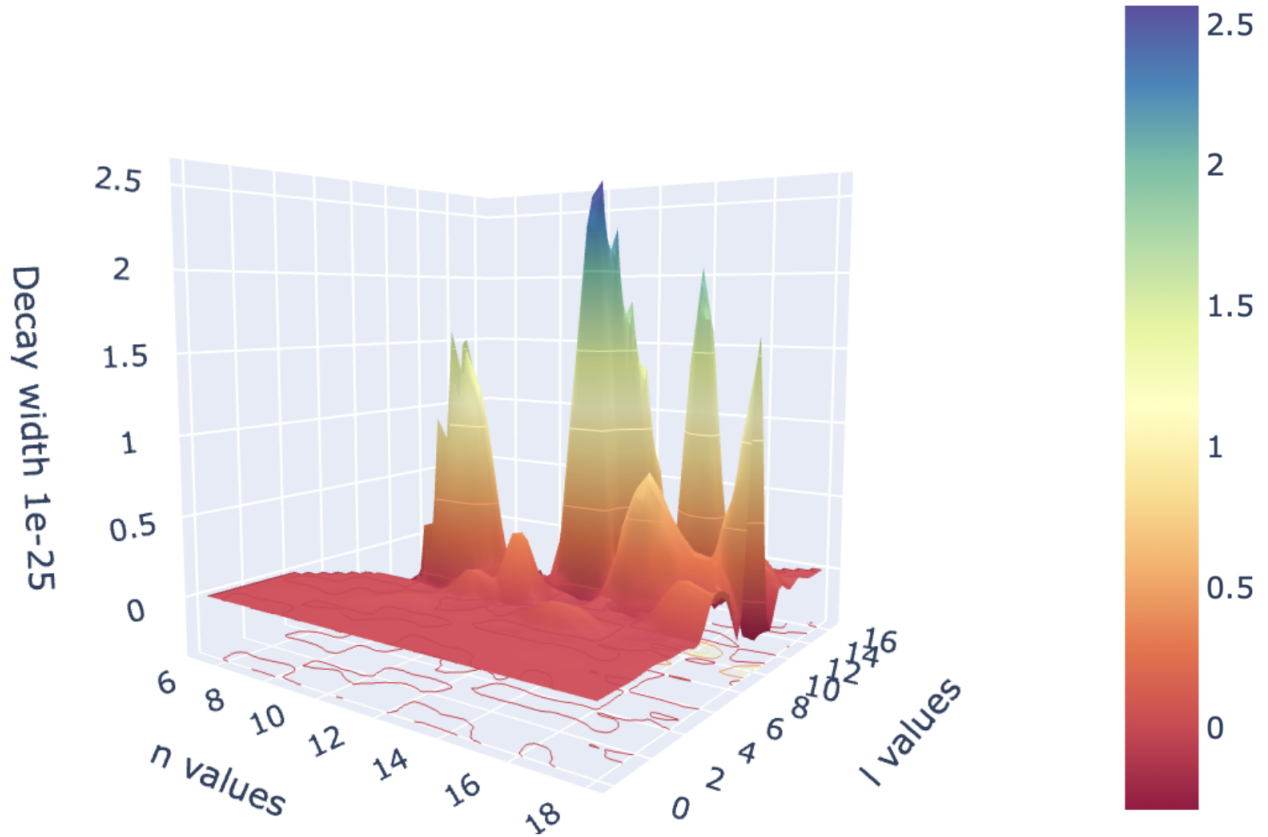


Figure 4.2: The interpolating surface serves just to guide the eye but only integer values of n , l make physical sense. The figure shows the 3D plot with the contour of transition decay width with respect to the n and l values of the final state of the muon. The peak represents the muon’s final state with the largest probability. The pion decays from $(n, l) = (17, 16)$ state.

4.4 PSI Experiment

Pionic helium is different from a normal helium atom; one of the electron from a normal helium atom is replaced by a negatively charged pion. Masaki Hori, Anna Soter, and his team designed an experiment at the PSI facility to do the laser spectroscopy of the pionic helium. They have observed an infrared transition of three-body pionic helium atoms by laser spectroscopy. With this experimental result, the precision of pion mass will increase by 2 – 3 orders of magnitude.

The proton beam from the PSI is used to hit a graphite target to produce the pion beam, which is then transported through an $E \times B$ Wien Filter to remove the e^- and μ^- contam-

ination from the produced π^- beam. The traversed π^- beam goes through a scintillation counter before stopping into the superfluid helium target. Most of the pion is absorbed by the helium nucleus, and a fraction of the pion beam produces the metastable pionic helium. The produced metastable pion is irradiated by an infrared laser to make a transition from $(n, l) = (17, 16)$ to $(n, l) = (17, 15)$ [35] and eventually absorbed by the helium nucleus. This causes the breakup of the nucleus, which can be detected. These pionic atoms can absorb or emit energy of discrete amounts, which can produce a quantum leap from one state to another. If the atom was present in the experiment tank and irradiated by the specific laser, then there will be the peak of nuclear fission fragments, and this is clear evidence of the existence of the atom [35].

Conclusion

In Chapter 2, by implementing mathematical technique, we derived the formula for the calculation of atomic form factor for non-equal masses and generalized direction of transferred momentum, which transformed the integral into a summation. Then the formula is implemented in Mathematica and Julia for the evaluation of the summation. From the Julia implementation, we developed a Julia package, which can be used to calculate the form factor using only the quantum numbers, the value of transferred momentum, the ratio of Bohr radii, and the direction of transferred momentum. The transition form factor formula and developed package can calculate any transition or decay form factors with transferred momentum in any direction or in the z -direction.

In Chapter 3, we reproduced the free pion decay rate calculation using Fermi's golden rule. In the first part of Chapter 4, we reproduced again the free pion decay rate calculation using the field-theoretic approach, which gives the lifetime of free pion 26ns. Then the same field theoretic approach is used to calculate the bound pion decay rate. With the form factor value from Chapter 2, we have calculated the decay rate of the bound pion and predicted that if the transition occurs from $(n, l) = (17, 16)$, then the final muon state $(14, 10)$ has the largest probability.

The future work, we can now easily find the X-ray energies that this muon will be emitting while falling to the ground state $1S$. This transition happens by electromagnetic interactions, so it happens rapidly with time, typically picoseconds (that time is on the order $\frac{1}{Z^4 \alpha^5 m_\mu}$), while the decay of the muon is caused by weak interactions, so it is a much slower process, and the muon lives on average $2.2\mu s$. Thus the muon can be treated like an almost stable particle and has enough time to fall to the ground state. The prediction of X-ray energies will allow our experimental colleagues to discover this transition from bound pion to bound muon.

Bibliography

- [1] M. Hori, A. Soter, H. Aghai-Khozani, D. Barna, A. Dax, R. Hayano, Y. Murakami, and H. Yamada, *Method for laser spectroscopy of metastable pionic helium atoms*, *Hyperfine Interactions* **233**, 83–87 (2015).
- [2] A. Alizzi, A. Sen, and Z. K. Silagadze, *Alternative implementation of atomic form factors*, *Acta Phys. Polon. B* **52**, 1209 (2021).
- [3] C. S. Ríos and J. S. Silva, *An implementation of atomic form factors*, *Computer Physics Communications* **151**, 79–88 (2003).
- [4] A. Uskov, A. Alizzi, and Z. Silagadze, *MuMuPy: A dimuonium-matter interaction calculator*, *Computer Physics Communications* **276** (2022).
- [5] H. Yukawa, *On the Interaction of Elementary Particles I*, *Proc. Phys. Math. Soc. Jap.* **17**, 48–57 (1935).
- [6] D. Bose and B. Choudhry, *Photographic plates as detectors of mesotron showers*, *Nature* **145**, 894–895 (1940).
- [7] D. Bose and B. Choudhuri, *Origin and nature of heavy ionization particles detected on photographic plates exposed to cosmic rays*, *Nature* **147**, 240–241 (1941).
- [8] D. Bose and B. Choudhuri, *A photographic method of estimating the mass of the mesotron*, *Nature* **148**, 259–260 (1941).
- [9] C. M. Lattes, H. Muirhead, G. P. Occhialini, and C. F. Powell, *Processes involving charged mesons*, *Nature* **159**, 694–697 (1947).
- [10] M. Conversi, E. Pancini, and O. Piccioni, *On the disintegration of negative mesons*, *Physical Review* **71**, 209 (1947).
- [11] H. A. Bethe, *Theory of the passage of fast corpuscular rays through matter*, *Annalen Phys.* **5**, 325–400 (1930).

- [12] K. Omidvar, *Bound-bound transitions in hydrogenlike atoms induced by fast charged particles*, Physical Review **188**, 140 (1969).
- [13] I.S. Gradshteyn and I.M. Ryzhik, *Table of integrals, series, and products*, Elsevier Science (2014).
- [14] H. S. W. Massey and C. Mohr, *The collision of slow electrons with atoms. iii.—the excitation and ionization of helium by electrons of moderate velocity*, Proceedings of the Royal Society of London. Series A, Containing Papers of a Mathematical and Physical Character **140**, 613–636 (1933).
- [15] A. Alizzi, A. Sen, and Z. Silagadze, *Alternative implementation of atomic form factors*, arXiv preprint arXiv:2107.07392 (2021).
- [16] G. Arfken, H. Weber, and F. Harris, *Mathematical methods for physicists: A comprehensive guide*, Academic Press, Amsterdam (2013).
- [17] R. S. Alassar, H. A. Mavromatis, and S. A. Sofianos, *A new integral involving the product of Bessel functions and associated Laguerre polynomials*, Acta Applicandae Mathematicae **100**, 263–267 (2007).
- [18] R. G. Newton, *Scattering theory of waves and particles*, Springer Science & Business Media (2013).
- [19] L. D. Landau and E. M. Lifshitz, *Quantum mechanics: non-relativistic theory*, Elsevier (2013).
- [20] A. R. Edmonds, *Angular momentum in quantum mechanics*, Princeton University Press (2016).
- [21] L. G. Afanasyev, *Form factors of the 1s, 2s, 3s, and 4s states of hydrogen-like atoms for discrete transitions*, Atomic Data and Nuclear Data Tables, 61(1), 31-33 (1995).
- [22] M. R. Flannery and D. Vrinceanu, *Classical and quantal atomic form factors for $n\ell m \rightarrow n'\ell' m$ transitions*, Phys. Rev. A **65** (2002).
- [23] D. Dewangan, *Asymptotic methods for Rydberg transitions*, Physics Reports **511**, 1–142 (2012).
- [24] J. W. Bezanson, S. Karpinski, V. B. Shah, and A. Edelman, *Julia: A fast dynamic language for technical computing*, arXiv preprint arXiv:1209.5145 (2012).

- [25] J. W. Bezanson, A. Edelman, S. Karpinski, and V. B. Shah, *Julia: A fresh approach to numerical computing*, SIAM Review **59**, 65–98 (2017).
- [26] J. M. Perkel, *Julia: come for the syntax, stay for the speed*, Nature **572**, 141–143 (2019).
- [27] J. W. Bezanson, *Abstraction in technical computing*, Ph.D. thesis, Massachusetts Institute of Technology (2015).
- [28] T. Arakaki, *FLoops.jl*, <https://github.com/JuliaFolds/FLoops.jl.git> (2020).
- [29] D. J. Griffiths, *Introduction to elementary particles; 2nd rev. version*, Wiley (2008).
- [30] M. Peskin, *Concepts of elementary particle physics*, Oxford Master Series in Condensed Matter Physics Series, Oxford University Press (2019).
- [31] P. Zyla et al., *Review of Particle Physics*, PTEP **2020**, 083C01 (2020).
- [32] E. Fermi and E. Teller, *The capture of negative mesotrons in matter*, Physical Review **72**, 399 (1947).
- [33] R. Feynman, *The theory of fundamental processes*, CRC Press (1961).
- [34] S. Coleman, *Lectures of Sidney Coleman on quantum field theory*, World Scientific (2018).
- [35] M. Hori, H. Aghai-Khozani, A. Sôtér, A. Dax, and D. Barna, *Laser spectroscopy of pionic helium atoms*, Nature **581** (2020).
- [36] D. J. Griffiths, *Introduction to quantum mechanics*, Pearson Prentice Hall, 2nd edition (2004).
- [37] J. J. Sakurai, *Advanced quantum mechanics*, Pearson Education (2006).

Appendix A

Form Factor Code

A.1 Mathematica Code for Integration

```
In[81]:= L[n_, m_, x_] := (n + m)! * Sum[(-1)^k * x^k / (k! * (n - k)! * (k + m)!), {k, 0, n}];  
Yp[l_, m_, e_, phi_] := Sqrt[(2 * l + 1) / (4 * Pi)] * Sqrt[(l - m)! / (l + m)!] * LegendreP[l, m, Cos[e]] * Exp[I * m * phi];  
  
psi2[n_, l_, m_, a_, r_] := (2 / (a^2 * n^2)) * Sqrt[(n - l - 1)! / (n + l)!] * Exp[-r / (a * n)] * (2 * r / (a * n))^l *  
L[n - l - 1, 2 * l + 1, (2 * r) / (a * n)] * Yp[l, m, e, 0];  
f6[n1_, l1_, m1_, n2_, l2_, rho_, q_] :=  
2 * Pi * Integrate[psi2[n2, l2, m1, rho, r] * r^2 * Sin[e] * Exp[I * q * r * Cos[e]] *  
psi2[n1, l1, m1, 1, r], {e, 0, Pi}, {r, 0, Infinity}];  
  
(* rho = a2/a1, m1 = m2 *)  
In[90]:= f6[5, 4, 3, 4, 3, 1.0, .66]  
Out[90]= 0. + 0.00398216 i
```

Figure A.1: Description of Mathematica code to calculate numerical integration. We have defined the wave function and the spherical harmonic function. *F6* function calculates the numerical integral.

```

In[ ]:= f8[n1_, l1_, m1_, ρ_, n2_, l2_, q_] :=
Module[{n = n1 - l1 - 1, δ = (n2 * ρ + n1) / (ρ * n1 * n2), ν = l + 1/2, γ = l1 + l2 + k + 3/2, α = 2 * l1 + 1},
N1 = 
$$\frac{(-1)^{m1+k+k1} 2^{l1+l2+k+k1-l+1}}{\rho^{\frac{3}{2}+l2} * n1^{2+l1+k1} * n2^{2+l2}} *$$


$$\sqrt{(\pi * (2 * l1 + 1) * (2 * l2 + 1) * \text{Gamma}[n1 + l1 + 1] * \text{Gamma}[n2 + l2 + 1] * \text{Gamma}[n1 - l1] * \text{Gamma}[n2 - l2])};$$

A1 = 
$$\frac{(I * q)^l * (2 * l + 1)}{\text{Gamma}[\nu + 1] * (\rho * n2)^k * \text{Gamma}[k + 1] * \text{Gamma}[2 * l2 + k + 2] * \text{Gamma}[n2 - l2 - k]}$$

ThreeJSymbol[{l1, 0}, {l2, 0}, {l, 0}] * ThreeJSymbol[{l1, m1}, {l2, -m1}, {l, 0}];
I1 = 
$$\frac{\text{Gamma}[\nu + \gamma + k1 + 1]}{\text{Gamma}[k1 + 1] * \text{Gamma}[n - k1 + 1] * \text{Gamma}[\alpha + k1 + 1] * \delta^{\nu + \gamma + k1 + 1}} *$$

Hypergeometric2F1[ $\frac{\nu + \gamma + k1 + 1}{2}$ ,  $\frac{\nu + \gamma + k1 + 2}{2}$ , 1 + ν,  $\frac{-q^2}{\delta^2}$ ];
temp1 = Sum[N1 * A1 * I1, {k, 0, n2 - l2 - 1}, {k1, 0, n}, {l, Abs[l1 - l2], l1 + l2}];
{temp1}
]

```

Figure A.2: Mathematica code to calculate the form factor using the Eq. (2.31).

A.2 Mathematica Code for Summation

A.3 Break Down of Mathematica Summation Calculation

The summation code in Mathematica starts to show problem while calculating the form factor for the combination of quantum numbers (10, 8, 7, 1, 8, 7, 0.66). Mathematica is giving the error which is given in figure (A.3). The result of the numerical integration is $-1.76983 \times 10^{-25} + i5.67761 \times 10^{-9}$. On the other hand, the result of the summation done in Julia is $0.0 + i5.677613206253347 \times 10^{-9}$.

A.4 The Name, Purpose, Usage and Output of Example Run

The FormFactor package is a Julia package to calculate atomic transition form factor. The code for this package can be found in the source code of the GitHub page <https://github.com/nuzhat07/FormFactor.jl.git>. A package contains modules, tests, and documentation. We use PkgTemplates.jl that helps us create all of these files and the configuration for a package. Before creating the package, we need to define a template that contains the initial configuration. First, we need to install PkgTemplates.jl. To install, we run the following

```
In[58]:= f8[10, 8, 7, 1, 8, 7, 0.66]
```

```
... Power: Infinite expression  $\frac{1}{0}$  encountered.  
... Infinity: Indeterminate expression  $\frac{0 \text{ ComplexInfinity}}{1415232000 \sqrt{1716099}}$  encountered.  
... Power: Infinite expression  $\frac{1}{0}$  encountered.  
... Infinity: Indeterminate expression  $\frac{0 \text{ ComplexInfinity}}{14370048000 \sqrt{117630786}}$  encountered.  
... Power: Infinite expression  $\frac{1}{0}$  encountered.  
... General: Further output of Power::infy will be suppressed during this calculation.  
... Infinity: Indeterminate expression  $\frac{0 \text{ ComplexInfinity}}{1307674368000 \sqrt{20036013}}$  encountered.  
... General: Further output of Infinity::indet will be suppressed during this calculation.
```

```
Out[58]= {Indeterminate}
```

Figure A.3: The error given by the Mathematica code A.2.

commands,

```
using Pkg  
Pkg.add("PkgTemplates")
```

Now, we can create our package template by executing the following commands:

```
using PkgTemplates  
t = Template(  
    user="your-GitHub-username",  
    license="MIT",  
    authors=["your-name"],  
    plugins=[Git(),  
            GitHubActions(),  
            ],  
)
```

Then, the following command will create our package.

```
t("YourPackageName")
```

Your package directory contains the following:

- LICENSE: The license that the package uses. For our package, we set the MIT license.
- Manifest.toml: It includes information on the package dependencies.
- Project.toml: It contains high-level information about the project.
- README.md: It contains information about our package. The README file has information on how to install our package and examples of how to use it.
- src: It contains the file Formfactor.jl. This is where we write the code for our package.
- test: It contains the file runtests.jl. This is where you write the code for testing your package.

src file has three .jl file, one of them is extra_form.jl file which calculates the form factor, another one is Formfactor.jl which is the main file of the package, and example.jl includes example code. extra_form.jl is imported into Formfactor.jl file. test file includes my_form_test.jl and runtests.jl. In my_form_test.jl, we have written the tests with a tolerance of 1/1000000.

To use the package in Julia REPL, we have to run following commands: Pkg is Julia's package manager. Pkg comes with a REPL. To get into the pkg> REPL, one needs to press] from the Julia REPL.

```
pkg> add https://github.com/nuzhat07/FormFactor.jl.git
```

To get back to the Julia REPL, press backspace or ^C.

```
1 julia> import FormFactor
2 julia> using FormFactor
3 julia> mform(3,2,-1,2,1,1.0,0.66)
4 0.19986502849251148
```

The mform function calculates the form factor for the assigned values. Also, one can check our test files from GitHub. By cloning the GitHub repository onto ones computer using URLs. One have to use the command git clone in the command line with the SSH or HTTPS URLs. To clone any GitHub repository one have to posses a GitHub account. There is another way to check our test files. One can download the ZIP file from the Download ZIP option and open the file in any standard IDE such as VS code or Atom and see the tests are passing or failing.

One can use this package to calculate a single form factor for given quantum numbers, the ratio of Bohr radii, and transferred momentum, an example given in the previous paragraph. Also, using the example.jl file from GitHub package, one can utilize a range of quantum numbers to calculate a list of form factors. After installing and importing the FormFactor package, one can check the output of the example.jl file or modify the file to get customized

output. To achieve this, one needs to download the ZIP file, which will be downloaded as FormFactor.jl-master. After unzipping the file, example.jl file can be found inside the src file. Then one has to run the following command *julia* in the command line, and drag and drop the example.jl in the terminal. Following is the output of example.jl file in the command line.

```
> julia example.jl
```

Screen output:

n1	l1	m1	n2	l2	form factor
1	0	0	1	0	0.8132334486398062
2	0	0	2	0	0.01711469127418809
2	1	0	2	1	-0.2773393490062824
2	1	1	2	1	0.3379867312677579
3	0	0	3	0	0.04332381544215912
3	1	0	3	1	0.06492183920351319
3	1	1	3	1	0.062487634226406505
3	2	0	3	2	0.14659853512409513
3	2	1	3	2	-0.19253685442347762
3	2	2	3	2	0.06505062969336908
4	0	0	4	0	0.02022506367731816
4	1	0	4	1	0.021695363145468622
4	1	1	4	1	0.020286498406379572
4	2	0	4	2	0.006071324630217897
4	2	1	4	2	-0.07112415772266187
4	2	2	4	2	0.032884238643133556
4	3	0	4	3	-0.06509529076544626
4	3	1	4	3	0.0658273037172201
4	3	2	4	3	-0.034513466856061326
4	3	3	4	3	0.006446826742729846
5	0	0	5	0	0.00887186658851675
5	1	0	5	1	0.0029606120661347887
5	1	1	5	1	0.00964488611800748
5	2	0	5	2	-0.014447821536305552

```

5 2 1 5 2 -0.028606890281786593
5 2 2 5 2 0.01721205791306006
5 3 0 5 3 -0.035665841642096366
5 3 1 5 3 0.04346734453047298
5 3 2 5 3 -0.026327906695564913
5 3 3 5 3 0.005262991878638247

...

10 9 6 10 9 -1.4191844167407435e-9
10 9 7 10 9 2.5543175809394167e-10
10 9 8 10 9 -2.8520799900826646e-11
10 9 9 10 9 1.4893597031965703e-12

```

To calculate the computation time, we used `example.jl` file in command line with command `> time julia example.jl`. The following Table A.1 contains the form factor value of various initial and final states using Julia, Fortran [3, 4], and numerical integration .

$n_1, l_1, m_1, n_2, l_2, \rho, q$	Julia	Fortran [3]	Fortran [4]	Numerical Integration
2, 1, 1, 2, 1, 1.0, 0.66	3.38e-1	3.03e-1	3.38e-1	3.38e-1
3, 2, 1, 4, 2, 1.0, 0.66	1.22e-1	3.78e-2	1.22e-1	1.22e-1
4, 2, 2, 3, 2, 1.0, .66	4.69e-2	3.25e-2	4.69e-2	4.69e-2
10, 9, 1, 9, 1, 1.0, .66	6.6e-7	6.24e-9	6.6e-7	6.6e-7
12, 5, 2, 11, 4, 1.0, 0.66	1.57e-3	2.48e-10	1.57e-3	1.57e-3

Table A.1: Absolute value of Form factors using different algorithms and different programming languages.

A.5 Julia Code

The `FormFactor` package is a Julia package to calculate atomic transition form factor. The code for this package can be found in the source code of the GitHub page <https://github.com/nuzhat07/FormFactor.jl.git>.

A.6 Modified `ffdiff.f` file used for comparison

The modified `ffdiff.f` file can be found in the readme file of the GitHub package <https://github.com/nuzhat07/FormFactor.jl.git>. We have modified the file with our desired

value of transferred momentum and range of quantum numbers to compare the computation time.

A.7 The main program

The `main.f` file is also added in the `readme` file of the GitHub package <https://github.com/nuzhat07/FormFactor.jl.git>. The main program of our interest has an array of two elements which indicates quantization axis along the direction of transferred momentum and the computation method 1 of [4], respectively. The `FTRANS` function is from `crsmumu.f` file of [4] package.

Appendix B

The Hydrogen Atom

B.1 The Schrödinger Equation for Hydrogen Atom

The time-independent Schrödinger equation in spherical coordinates is [36]

$$\left(-\frac{\hbar^2}{2m}\nabla^2 + V(r)\right)\psi(r, \theta, \phi) = E\psi(r, \theta, \phi), \quad (\text{B.1})$$

where the Laplacian, $\nabla^2 = \frac{1}{r^2}\frac{\partial}{\partial r}\left(r^2\frac{\partial}{\partial r}\right) + \frac{1}{r^2}\frac{1}{\sin\theta}\frac{\partial}{\partial\theta}\left(\sin\theta\frac{\partial}{\partial\theta}\right) + \frac{1}{(r\sin\theta)^2}\frac{\partial^2}{\partial\phi^2}$, in spherical coordinates. The solution of the Schrödinger equation is of the form $\psi(r, \theta, \phi) = R(r)Y(\theta, \phi)$. Substituting it into the Eq. (B.1) and dividing by $\frac{\hbar^2 R Y}{2mr^2}$ we get,

$$\left[\frac{1}{R}\frac{d}{dr}\left(r^2\frac{dR}{dr}\right) - \frac{2mr^2}{\hbar^2}(V(r) - E)\right] + \frac{1}{Y}\left[\frac{1}{\sin\theta}\frac{\partial}{\partial\theta}\left(\sin\theta\frac{\partial Y}{\partial\theta}\right) + \frac{1}{\sin^2\theta}\frac{\partial^2 Y}{\partial\phi^2}\right] = 0. \quad (\text{B.2})$$

The first term of the equation depends on r , and the second term on θ and ϕ . So Eq. (B.2) can be valid if and only if

$$\begin{aligned} \frac{1}{R}\frac{d}{dr}\left(r^2\frac{dR}{dr}\right) - \frac{2mr^2}{\hbar^2}(V(r) - E) &= l(l+1), \\ \frac{1}{Y}\left[\frac{1}{\sin\theta}\frac{\partial}{\partial\theta}\left(\sin\theta\frac{\partial Y}{\partial\theta}\right) + \frac{1}{\sin^2\theta}\frac{\partial^2 Y}{\partial\phi^2}\right] &= -l(l+1), \end{aligned} \quad (\text{B.3})$$

where $l(l+1)$ is a constant. The first equation is the Radial equation, and the second equation is the Angular equation. The solution of the Angular equation is the spherical harmonics.

To solve the radial part, let us make a transformation from $R(r)$ to $u(r)$, where

$$R = \frac{u}{r}, \quad \frac{dR}{dr} = \frac{1}{r^2} \left(r \frac{du}{dr} - u \right) \\ \frac{d}{dr} \left(r^2 \frac{dR}{dr} \right) = r \frac{d^2u}{dr^2}. \quad (\text{B.4})$$

So the radial equation becomes, after multiplying $-\frac{\hbar^2}{2mr}$

$$-\frac{\hbar^2}{2m} \frac{d^2u(r)}{dr^2} + \left[V(r) + \frac{\hbar^2}{2m} \frac{l(l+1)}{r^2} \right] u(r) = Eu(r). \quad (\text{B.5})$$

This equation is similar to the 1-dimensional Schrödinger equation in variable r with effective potential

$$V_{eff}(r) = V(r) + \frac{\hbar^2 l(l+1)}{2mr^2}. \quad (\text{B.6})$$

The Hydrogen atom is a two-body system with an electron of charge $-e$, circulating the heavier proton of charge $+e$. Since the mass of the electron is much lighter compared to the proton, then the system can be reduced to a single particle system. The potential energy of the electron due to the proton can be found from Coulomb's law,

$$V(r) = -\frac{e^2}{4\pi\epsilon_0 r}. \quad (\text{B.7})$$

Here, we will consider only bound states with $E < 0$. As $V(r) \rightarrow 0$ with $r \rightarrow \infty$ the system will have a continuum spectrum for $E \geq 0$.

Let us define

$$k \equiv \frac{\sqrt{-2mE}}{\hbar}, \quad (\text{B.8})$$

the radial equation becomes

$$\frac{1}{k^2} \frac{d^2u}{dr^2} = \left[1 - \frac{me^2}{2\pi\epsilon_0 \hbar^2 k} \frac{1}{(kr)} + \frac{l(l+1)}{(kr)^2} \right] u. \quad (\text{B.9})$$

Introducing a new parameter

$$\rho \equiv kr, \quad \rho_0 \equiv \frac{me^2}{2\pi\epsilon_0 \hbar^2 k}. \quad (\text{B.10})$$

We get a simpler equation

$$\frac{d^2u}{d\rho^2} = \left(1 - \frac{\rho_0}{\rho} + \frac{l(l+1)}{\rho^2} \right) u. \quad (\text{B.11})$$

The next step is to find the asymptotic behavior of the solution at the boundaries. At $\rho \rightarrow \infty$,

the constant term in the brackets dominates and we are left with,

$$\frac{d^2u}{d\rho^2} = u. \quad (\text{B.12})$$

The general solution is

$$u(\rho) = Ae^{-\rho} + Be^{\rho}, \quad (\text{B.13})$$

but e^{ρ} blows up as $\rho \rightarrow \infty$, so $B = 0$ and

$$u(\rho) \approx Ae^{-\rho}, \quad (\text{B.14})$$

for large ρ . And as $\rho \rightarrow 0$,

$$\frac{d^2u}{d\rho^2} \approx \frac{l(l+1)}{\rho^2}u. \quad (\text{B.15})$$

The general solution is

$$u(\rho) = C\rho^{l+1} + D\rho^{-l}, \quad (\text{B.16})$$

but ρ^{-l} blows up as $\rho \rightarrow 0$, so $D = 0$. Thus

$$u(\rho) \approx C\rho^{l+1}, \quad (\text{B.17})$$

for small ρ . Factoring out the asymptotic functions the solution becomes

$$u(\rho) = \rho^{l+1}e^{-\rho}v(\rho). \quad (\text{B.18})$$

Let us calculate the second derivative of $u(\rho)$

$$\frac{du}{d\rho} = \rho^l e^{-\rho} \left[(l+1-\rho)v + \rho \frac{dv}{d\rho} \right], \quad (\text{B.19})$$

and

$$\frac{d^2u}{d\rho^2} = \rho^l e^{-\rho} \left(\left[-2l - 2 + \rho + \frac{l(l+1)}{\rho} \right] v + 2(l+1-\rho) \frac{dv}{d\rho} + \rho \frac{d^2v}{d\rho^2} \right). \quad (\text{B.20})$$

Let us now substitute these in the Eq. (B.9)

$$\rho \frac{d^2v}{d\rho^2} + 2(l+1-\rho) \frac{dv}{d\rho} + [\rho - 2(l+1)]v = 0. \quad (\text{B.21})$$

This is so-called ‘‘hyper-geometric’’ equation. The $v(\rho)$ can be expressed as a power series in

ρ ,

$$v(\rho) = \sum_{j=0}^{\infty} c_j \rho^j. \quad (\text{B.22})$$

Differentiating term by term

$$\frac{dv}{d\rho} = \sum_{j=0}^{\infty} j c_j \rho^{j-1} = \sum_{j=0}^{\infty} (j+1) c_{j+1} \rho^j. \quad (\text{B.23})$$

Differentiating again,

$$\frac{d^2v}{d\rho^2} = \sum_{j=0}^{\infty} j(j+1) c_{j+1} \rho^{j-1}. \quad (\text{B.24})$$

Inserting these into Eq. (B.21), we have

$$\sum_{j=0}^{\infty} j(j+1) c_{j+1} \rho^j + 2(l+1) \sum_{j=0}^{\infty} (j+1) c_{j+1} \rho^j - 2 \sum_{j=0}^{\infty} j c_j \rho^j + [\rho_o - 2(l+1)] \sum_{j=0}^{\infty} c_j \rho^j = 0. \quad (\text{B.25})$$

Equating the coefficients of like powers produces,

$$j(j+1) c_{j+1} + 2(l+1)(j+1) c_{j+1} - 2j c_j + [\rho_o - 2(l+1)] c_j = 0. \quad (\text{B.26})$$

Or,

$$c_{j+1} = \frac{2(j+l+1) - \rho_o}{(j+1)(j+2l+2)} c_j, \quad (\text{B.27})$$

this is the recursion formula which determines the coefficients. To get a polynomial of degree n_r the recursion should stop at $j = n_r$. So that

$$c_{n_r+1} = 0, \quad (\text{B.28})$$

which means that

$$2(n_r + l + 1) - \rho_o = 0. \quad (\text{B.29})$$

Defining

$$n \equiv n_r + l + 1, \quad (\text{B.30})$$

where n is the so-called ‘‘principle quantum number’’ and n_r is the ‘‘radial quantum number’’,

$$\rho_o = 2n. \quad (\text{B.31})$$

Since $n_r = 0, 1, 2, \dots$ and $l = 0, 1, 2, \dots$, the principle quantum number is positive integer

$n = 1, 2, \dots$. We can have energy E from Eq. (B.8)

$$\begin{aligned} E &= -\frac{\hbar^2 k^2}{2m} \\ &= -\frac{\hbar^2}{2m} \left(\frac{me^2}{4\pi\epsilon_0\hbar^2 n} \right)^2 \\ &= -\frac{mc^2\alpha^2}{2(n_r + l + 1)^2} \end{aligned} \quad (\text{B.32})$$

where $\alpha = \frac{e^2}{4\pi\epsilon_0\hbar c} = \frac{1}{137}$ which is the fine structure constant. Combining Eq. (B.10) and Eq. (B.31)

$$k = \left(\frac{me^2}{4\pi\epsilon_0\hbar^2} \right) \frac{1}{n} = \frac{1}{an} \quad (\text{B.33})$$

where

$$a \equiv \frac{4\pi\epsilon_0\hbar^2}{me^2} \quad (\text{B.34})$$

is the Bohr Radius and

$$a = \frac{\hbar}{\alpha mc}. \quad (\text{B.35})$$

The spatial wave function for Hydrogen atom is

$$\psi_{nlm}(r, \theta, \phi) = R_{nl}(r)Y_l^m(\theta, \phi), \quad (\text{B.36})$$

where

$$R_{nl}(r) = \frac{1}{r} \rho^{l+1} e^{-\rho} v(\rho), \quad (\text{B.37})$$

and $v(\rho)$ is a polynomial of degree $n_r = n - l - 1$, the coefficients of $v(\rho)$ are determined by

$$c_{j+1} = \frac{2(j+l+1-n)}{(j+1)(j+2l+2)} c_j. \quad (\text{B.38})$$

Since $n \equiv n_r + l + 1$, the ground state of hydrogen has $l = 0$ and $m = 0$. So

$$\psi_{100}(r, \theta, \phi) = R_{10}(r)Y_0^0(\theta, \phi). \quad (\text{B.39})$$

With $j = 0$, $v(\rho)$ is a constant

$$R_{10}(r) = \frac{c_0}{a} e^{-r/a}. \quad (\text{B.40})$$

The normalization constant

$$\int_0^\infty |R_{10}(r)|^2 r^2 dr = \frac{|c_0|^2}{a^2} \int_0^\infty e^{-2r/a} r^2 dr = |c_0|^2 \frac{a}{4} = 1. \quad (\text{B.41})$$

So $c_o = \frac{2}{\sqrt{a}}$. And $Y_0^0 = \frac{1}{\sqrt{4\pi}}$, so the ground state wave function of hydrogen atom is

$$\psi_{100}(r, \theta, \phi) = \frac{1}{\sqrt{\pi a^3}} e^{-r/a}. \quad (\text{B.42})$$

We also can determine R_{nl} using special function, $v(\rho)$ is a polynomial of degree n_r

$$v(\rho) = L_{n_r}^{2l+1}(2\rho) = L_{n-l-1}^{2l+1}(2\rho), \quad (\text{B.43})$$

where

$$L_{q-p}^p(x) \equiv (-1)^p \left(\frac{d}{dx} \right)^p L_q(x), \quad (\text{B.44})$$

is an associated Laguerre polynomial and

$$L_q(x) \equiv e^x \left(\frac{d}{dx} \right)^q (e^{-x} x^q), \quad (\text{B.45})$$

is the q^{th} Laguerre polynomial. Finally, the wave function can be written as

$$\psi_{nlm}(r, \theta, \phi) = A_r e^{-r/na} \left(\frac{2r}{na} \right)^l [L_{n-l-1}^{2l+1}(2r/na)] Y_l^m(\theta, \phi), \quad (\text{B.46})$$

where A_r is the normalization constant.

B.2 The Klein-Gordon Equation for Hydrogen Atom

The Klein Gordon equation for free particle is

$$\partial_\mu \partial^\mu \psi + m^2 \psi = 0, \quad (\text{B.47})$$

where $\partial_\mu \partial^\mu = \frac{\partial^2}{\partial t^2} - \vec{\nabla}^2$. The Coulomb potential is incorporated in the Klein-Gordon equation by minimal coupling. To solve the Klein-Gordon equation for the hydrogen atom we will be using $U(1)$ gauge covariant Klein-Gordon equation. If a globally $U(1)$ symmetric theory couples to a gauge field A_μ by the covariant derivative $\partial_\mu \rightarrow D_\mu \equiv \partial_\mu + iQA_\mu$ where Q is charge, a locally symmetric $U(1)$ theory is appeared. This way of coupling a gauge potential to a matter field is called principle of minimal coupling [29]. The gauge covariant Klein-Gordon equation is

$$D_\mu D^\mu \psi + \frac{m^2 c^2}{\hbar^2} \psi = 0. \quad (\text{B.48})$$

Here $D_\mu = \partial_\mu - \frac{ie}{\hbar c} A_\mu$. Since the system is a hydrogen atom and the potential is Coulomb

potential, it can be represented as a four-vector with the zeroth component as Coulomb potential and the rest of the components zero.

$$A_\mu = \begin{pmatrix} \frac{Ze}{4\pi\epsilon_0 r} \\ 0 \\ 0 \\ 0 \end{pmatrix}. \quad (\text{B.49})$$

Using the property of four vector and the above A_μ we have the Klein-Gordon equation for the hydrogen atom,

$$\left(\frac{1}{c} \frac{\partial}{\partial t} - i \frac{Ze^2}{4\pi\epsilon_0 \hbar c r} \right)^2 \psi - \nabla^2 \psi + \frac{m^2 c^2}{\hbar^2} \psi = 0 \quad (\text{B.50})$$

$$-c^2 \nabla^2 \psi + \frac{m^2 c^4}{\hbar^2} \psi = \left(i \frac{\partial}{\partial t} + c \frac{Z\alpha}{r} \right)^2 \psi \quad (\text{B.51})$$

$$-c^2 \hbar^2 \nabla^2 \psi + m^2 c^4 \psi = \left(i \hbar \frac{\partial}{\partial t} + \hbar c \frac{Z\alpha}{r} \right)^2 \psi. \quad (\text{B.52})$$

Here $\alpha = \frac{e^2}{4\pi\epsilon_0 \hbar c}$. Energy operator has a form from the wave-function $\psi = e^{i(kx - \omega t)}$ and $E = \hbar\omega$,

$$i \hbar \frac{\partial \psi}{\partial t} = E \psi. \quad (\text{B.53})$$

Inserting this into Eq. (B.52) gives

$$-c^2 \hbar^2 \nabla^2 \psi + m^2 c^4 \psi = \left(E + \hbar c \frac{Z\alpha}{r} \right)^2 \psi. \quad (\text{B.54})$$

Since Coulomb potential is a spherically symmetric potential, the Laplacian, ∇^2 in Eq. (B.54) should be in spherical coordinate

$$\nabla^2 = \frac{1}{r^2} \frac{\partial}{\partial r} \left(r^2 \frac{\partial}{\partial r} \right) + \frac{1}{r^2 \sin \theta} \frac{\partial}{\partial \theta} \left(\sin \theta \frac{\partial}{\partial \theta} \right) + \frac{1}{r^2 \sin^2 \theta} \frac{\partial^2}{\partial \phi^2}. \quad (\text{B.55})$$

The Laplacian from Eq. (B.55) putting into Eq. (B.54)

$$\begin{aligned}
& -c^2\hbar^2 \left(\frac{1}{r^2} \frac{\partial}{\partial r} \left(r^2 \frac{\partial \psi}{\partial r} \right) + \frac{1}{r^2 \sin \theta} \frac{\partial}{\partial \theta} \left(\sin \theta \frac{\partial \psi}{\partial \theta} \right) + \frac{1}{r^2 \sin^2 \theta} \frac{\partial^2 \psi}{\partial \phi^2} \right) + \\
m^2 c^4 \psi &= \left(E + \hbar c \frac{Z\alpha}{r} \right)^2 \psi
\end{aligned} \tag{B.56}$$

$$\begin{aligned}
& \frac{1}{r^2} \frac{\partial}{\partial r} \left(r^2 \frac{\partial \psi}{\partial r} \right) + \frac{1}{r^2 \sin \theta} \frac{\partial}{\partial \theta} \left(\sin \theta \frac{\partial \psi}{\partial \theta} \right) + \frac{1}{r^2 \sin^2 \theta} \frac{\partial^2 \psi}{\partial \phi^2} - \frac{m^2 c^2}{\hbar^2} \psi \\
& + \left(\frac{E}{c\hbar} + \frac{Z\alpha}{r} \right)^2 \psi = 0
\end{aligned} \tag{B.57}$$

$$\frac{\partial}{\partial r} \left(r^2 \frac{\partial \psi}{\partial r} \right) - r^2 \frac{m^2 c^2}{\hbar^2} \psi + r^2 \left(\frac{E}{c\hbar} + \frac{Z\alpha}{r} \right)^2 \psi = -\frac{1}{\sin \theta} \frac{\partial}{\partial \theta} \left(\sin \theta \frac{\partial \psi}{\partial \theta} \right) - \frac{1}{\sin^2 \theta} \frac{\partial^2 \psi}{\partial \phi^2}. \tag{B.58}$$

To do the separation of variables introducing $\psi = Y(\theta, \phi)R(r)$ and dividing by YR

$$\begin{aligned}
\frac{1}{R} \frac{d}{dr} \left(r^2 \frac{dR}{dr} \right) - r^2 \frac{m^2 c^2}{\hbar^2} + r^2 \left(\frac{E}{c\hbar} + \frac{Z\alpha}{r} \right)^2 = \\
-\frac{1}{Y \sin \theta} \frac{\partial}{\partial \theta} \left(\sin \theta \frac{\partial Y}{\partial \theta} \right) - \frac{1}{Y \sin^2 \theta} \frac{\partial^2 Y}{\partial \phi^2},
\end{aligned} \tag{B.59}$$

which gives two separated equations equals to some constant

$$\frac{1}{R} \frac{d}{dr} \left(r^2 \frac{dR}{dr} \right) - r^2 \frac{m^2 c^2}{\hbar^2} + r^2 \left(\frac{E}{c\hbar} + \frac{Z\alpha}{r} \right)^2 = l(l+1) \tag{B.60}$$

$$-\frac{1}{Y \sin \theta} \frac{\partial}{\partial \theta} \left(\sin \theta \frac{\partial Y}{\partial \theta} \right) - \frac{1}{Y \sin^2 \theta} \frac{\partial^2 Y}{\partial \phi^2} = l(l+1). \tag{B.61}$$

The angular equation

$$\frac{1}{\sin \theta} \frac{\partial}{\partial \theta} \left(\sin \theta \frac{\partial Y}{\partial \theta} \right) + \frac{1}{\sin^2 \theta} \frac{\partial^2 Y}{\partial \phi^2} + l(l+1)Y = 0. \tag{B.62}$$

The angular equation is the same as the Schrödinger equation so the normalized angular wave functions are called spherical harmonics

$$Y_l^m(\theta, \phi) = \epsilon \sqrt{\frac{(2l+1)(l-|m|)!}{4\pi(l+|m|)!}} e^{im\phi} P_l^m(\cos \theta), \tag{B.63}$$

where $\epsilon = (-1)^m$ for $m \geq 0$ and $\epsilon = 1$ for $m \leq 0$, $P_l^m(x) = (-1)^m (1-x^2)^{m/2} \frac{d^m}{dx^m} P_l(x)$, $P_l^{-m}(x) = (-1)^m \frac{(l-m)!}{(l+m)!} P_l^m(x)$, $P_l(x) = \frac{1}{2^l l!} \frac{d^l}{dx^l} (x^2-1)^l$, $-l \leq m \leq l$.

The radial equation of the Klein-Gordon equation starts to deviate from the Schrödinger equation

$$\frac{1}{r^2} \frac{d}{dr} \left(r^2 \frac{dR}{dr} \right) + \left[\left(\frac{E}{\hbar c} + \frac{Z\alpha}{r} \right)^2 - \frac{m^2 c^2}{\hbar^2} - \frac{l(l+1)}{r^2} \right] R = 0 \quad (\text{B.64})$$

$$\left[\frac{1}{r^2} \frac{d}{dr} \left(r^2 \frac{d}{dr} \right) + \frac{E^2}{\hbar^2 c^2} + \frac{2E}{\hbar c} \frac{Z\alpha}{r} - \frac{m^2 c^2}{\hbar^2} + \frac{Z^2 \alpha^2 - l(l+1)}{r^2} \right] R = 0. \quad (\text{B.65})$$

Substituting

$$R = \frac{u}{r}, \quad (\text{B.66})$$

and

$$\frac{dR}{dr} = \frac{1}{r} \frac{du}{dr} - \frac{u}{r^2} \quad (\text{B.67})$$

$$\frac{1}{r^2} \frac{d}{dr} \left(r^2 \frac{dR}{dr} \right) = \frac{1}{r} \frac{d^2 u}{dr^2}. \quad (\text{B.68})$$

Eq. (B.65) becomes

$$\left[\frac{d^2}{dr^2} - \frac{l(l+1) - Z^2 \alpha^2}{r^2} + \frac{2ZE\alpha}{\hbar cr} - \frac{m^2 c^4 - E^2}{\hbar^2 c^2} \right] u = 0. \quad (\text{B.69})$$

To make the equation more convenient introducing new parameter, $\beta = 2 \frac{(m^2 c^4 - E^2)^{\frac{1}{2}}}{\hbar c}$

$$\left[\frac{d^2}{dr^2} - \frac{l^2 + l + \frac{1}{4} - Z^2 \alpha^2 - \frac{1}{4}}{r^2} + \frac{2ZE\alpha}{\hbar cr} - \frac{\beta^2}{4} \right] u = 0 \quad (\text{B.70})$$

$$\left[\frac{d^2}{dr^2} - \frac{(l + \frac{1}{2})^2 - Z^2 \alpha^2 - \frac{1}{4}}{r^2} + \frac{2ZE\alpha}{\hbar cr} - \frac{\beta^2}{4} \right] u = 0, \quad (\text{B.71})$$

and another parameter $\mu = \sqrt{(l + \frac{1}{2})^2 - Z^2 \alpha^2}$

$$\left[\frac{d^2}{dr^2} - \frac{\mu^2 - \frac{1}{4}}{r^2} + \frac{2ZE\alpha}{\hbar cr} - \frac{\beta^2}{4} \right] u = 0 \quad (\text{B.72})$$

$$\left[\frac{1}{\beta^2} \frac{d^2}{dr^2} - \frac{\mu^2 - \frac{1}{4}}{r^2 \beta^2} + \frac{2ZE\alpha}{\hbar c \beta} \frac{1}{\beta r} - \frac{1}{4} \right] u = 0. \quad (\text{B.73})$$

Let's make another substitution,

$$\rho = \beta r, \lambda = \frac{2ZE\alpha}{\hbar c\beta}, \quad w(\rho) = w(\beta r) = u(r), \quad (\text{B.74})$$

which gives

$$\left[\frac{d^2}{d\rho^2} - \frac{\mu^2 - \frac{1}{4}}{\rho^2} + \frac{\lambda}{\rho} - \frac{1}{4} \right] w(\rho) = 0. \quad (\text{B.75})$$

Next we examine the asymptotic form of the solutions. For the case of large ρ

$$\frac{d^2 w}{d\rho^2} = \frac{1}{4} w. \quad (\text{B.76})$$

The general solution is:

$$w = Ae^{-\frac{\rho}{2}} + Be^{\frac{\rho}{2}}, \quad (\text{B.77})$$

but e^{ρ} blows up (as $\rho \rightarrow \infty$) so $B = 0$. Evidently

$$w \sim Ae^{-\frac{\rho}{2}}. \quad (\text{B.78})$$

For the case of small ρ

$$\frac{d^2 w}{d\rho^2} = \frac{\mu^2 - \frac{1}{4}}{\rho^2} w. \quad (\text{B.79})$$

The general solution of this equation is:

$$w = A\rho^{\frac{1}{2}+\mu} + B\rho^{\frac{1}{2}-\mu}. \quad (\text{B.80})$$

The second term is not normalizable, so $B = 0$. Therefore, the desired asymptotic form is:

$$w \sim \rho^{\frac{1}{2}+\mu}. \quad (\text{B.81})$$

Peeling off the asymptotic behavior, introducing the new function $v(\rho)$:

$$w = \rho^{\frac{1}{2}+\mu} e^{-\frac{\rho}{2}} v(\rho). \quad (\text{B.82})$$

First derivative of w

$$\frac{dw}{d\rho} = \left(\frac{1}{2} + \mu \right) \rho^{\mu-\frac{1}{2}} e^{-\frac{\rho}{2}} v(\rho) - \frac{1}{2} \rho^{\frac{1}{2}+\mu} e^{-\frac{\rho}{2}} v(\rho) + \rho^{\frac{1}{2}+\mu} e^{-\frac{\rho}{2}} \frac{dv(\rho)}{d\rho}. \quad (\text{B.83})$$

Taking the second derivative of w

$$\frac{d^2 w}{d\rho^2} = \rho^{\frac{1}{2}+\mu} e^{-\frac{\rho}{2}} \left[\frac{\mu^2 - \frac{1}{4}}{\rho^2} v - \left(\frac{1}{2} + \mu \right) \frac{1}{\rho} v + 2 \left(\frac{1}{2} + \mu \right) \frac{1}{\rho} \frac{dv}{d\rho} + \frac{1}{4} v - \frac{dv}{d\rho} + \frac{d^2 v}{d\rho^2} \right]. \quad (\text{B.84})$$

With the value of the second derivative of w , the radial equation reads

$$\left[\frac{\mu^2 - \frac{1}{4}}{\rho^2} v - \left(\frac{1}{2} + \mu \right) \frac{1}{\rho} v + 2 \left(\frac{1}{2} + \mu \right) \frac{1}{\rho} \frac{dv}{d\rho} + \frac{1}{4} v - \frac{dv}{d\rho} + \frac{d^2 v}{d\rho^2} - \frac{\mu^2 - \frac{1}{4}}{\rho^2} v + \frac{\lambda}{\rho} v - \frac{1}{4} v \right] \times \rho^{\frac{1}{2}+\mu} e^{-\frac{\rho}{2}} = 0 \quad (\text{B.85})$$

$$\left(\frac{1}{2} + \mu \right) \frac{1}{\rho} v - 2 \left(\frac{1}{2} + \mu \right) \frac{1}{\rho} \frac{dv}{d\rho} + \frac{dv}{d\rho} - \frac{d^2 v}{d\rho^2} - \frac{\lambda}{\rho} v = 0. \quad (\text{B.86})$$

Now again defining few new constants

$$b = \mu + \frac{1}{2} - \lambda, \quad d = 2\mu + 1, \quad (\text{B.87})$$

$$\frac{d^2 v}{d\rho^2} + \left(\frac{d}{\rho} - 1 \right) \frac{dv}{d\rho} - \frac{b}{\rho} v = 0. \quad (\text{B.88})$$

Using power series for finding solutions

$$v(\rho) = \sum_{j=0}^{\infty} c_j \rho^j, \quad (\text{B.89})$$

and differentiating

$$\frac{dv}{d\rho} = \sum_{j=0}^{\infty} j c_j \rho^{j-1}, \quad (\text{B.90})$$

differentiating again,

$$\frac{d^2 v}{d\rho^2} = \sum_{j=0}^{\infty} j(j-1) c_j \rho^{j-2}. \quad (\text{B.91})$$

Inserting these into equation Eq. (B.88), we have

$$\sum_{j=0}^{\infty} j(j-1)c_j\rho^{j-2} + d\sum_{j=0}^{\infty} jc_j\rho^{j-2} - \sum_{j=0}^{\infty} jc_j\rho^{j-1} - b\sum_{j=0}^{\infty} c_j\rho^{j-1} = 0 \quad (\text{B.92})$$

$$\sum_{j=0}^{\infty} [j(j+1)c_{j+1} + d(j+1)c_{j+1} - jc_j - bc_j] \rho^{j-1} = 0. \quad (\text{B.93})$$

The recursion relation yields by equating the coefficients of same powers,

$$c_{j+1} = \frac{j+b}{j(j+1)+d(j+1)}c_j \quad (\text{B.94})$$

$$c_j = \frac{b+j-1}{j(d+j-1)}c_{j-1}. \quad (\text{B.95})$$

Now for large j , the coefficient is

$$c_{j+1} \approx \frac{1}{j}c_j. \quad (\text{B.96})$$

Therefore,

$$c_j = \frac{1}{j!}c_0, \quad (\text{B.97})$$

so

$$v(\rho) = \sum_{j=0}^{\infty} c_j\rho^j = c_0 \sum_{j=0}^{\infty} \frac{1}{j!}\rho^j = c_0 e^\rho. \quad (\text{B.98})$$

To terminate the series there must occur some maximal integer, $j = n_r$:

$$c_{n_r+1} = 0. \quad (\text{B.99})$$

From the recursion relation

$$b + n_r = 0, \quad (\text{B.100})$$

where n_r is a non-negative integer the so called radial quantum number. Replacing b

$$b + n_r = \mu + \frac{1}{2} - \lambda + n_r = 0, \quad (\text{B.101})$$

again replacing μ and λ and β ,

$$\sqrt{\left(l + \frac{1}{2}\right)^2 - Z^2\alpha^2} + \frac{1}{2} + n_r = \lambda = \frac{2Z\alpha E}{\hbar c\beta} = \frac{2Z\alpha E}{2(m^2c^4 - E^2)^{\frac{1}{2}}} \quad (\text{B.102})$$

$$\sqrt{\left(l + \frac{1}{2}\right)^2 - Z^2\alpha^2} + \frac{1}{2} + n_r = \frac{2Z\alpha E}{2(m^2c^4 - E^2)^{\frac{1}{2}}}. \quad (\text{B.103})$$

By manipulating the last equation we have the energy,

$$E = mc^2 \left(1 + \frac{Z^2\alpha^2}{\left(n_r + \frac{1}{2} + \sqrt{\left(l + \frac{1}{2}\right)^2 - Z^2\alpha^2}\right)^2} \right)^{-\frac{1}{2}} \quad (\text{B.104})$$

Defining, $n = n_r + l + 1$ the principal quantum number, the energy equation becomes,

$$E = mc^2 \left(1 + \frac{Z^2\alpha^2}{\left(n - l - \frac{1}{2} + \sqrt{\left(l + \frac{1}{2}\right)^2 - Z^2\alpha^2}\right)^2} \right)^{-\frac{1}{2}} \quad (\text{B.105})$$

The radial wave function is

$$R(r) = A_r \frac{1}{r} (\beta r)^{\frac{1}{2} + \sqrt{\left(l + \frac{1}{2}\right)^2 - Z^2\alpha^2}} e^{-\frac{\beta r}{2}} v_{nl}(\beta r) \quad (\text{B.106})$$

where, A_r is the normalization constant and $v_{nl}(\beta r) = v_{nl}(\rho)$ is a polynomial of degree $n_r = n - l - 1$. The complete wave function therefore is

$$\psi = A_r \frac{1}{r} (\beta r)^{\frac{1}{2} + \sqrt{\left(l + \frac{1}{2}\right)^2 - Z^2\alpha^2}} e^{-\frac{\beta r}{2}} v_{nl}(\beta r) Y_l^m(\theta, \phi) \quad (\text{B.107})$$

A_r is the normalization constant. The Klein-Gordon equation does not perfectly describe the hydrogen atom. Because this equation is ideal for relativistic scalar, but the electron is not a relativistic scalar. The normalization constant is

$$A_r = \frac{ch\Gamma\left(\sqrt{4l^2 + 4l - 4Z^2\alpha^2} + 1 + 2\right)}{2 \sqrt{c^4m^2 - \frac{c^4m^2}{\alpha^2 Z^2} \left(\sqrt{l^2 + l - \alpha^2 Z^2 + \frac{1}{4}} - l + n - \frac{1}{2}\right)^2 + 1}} \quad (\text{B.108})$$

B.3 Dirac Equation for Hydrogen Atom: Ground State

The Dirac equation is [37]

$$\left(\gamma_\mu \frac{\partial}{\partial x_\mu} + \frac{mc}{\hbar} \right) \psi = 0, \quad (\text{B.109})$$

where γ_μ with $\mu = 1, 2, 3, 4$ are 4×4 matrices given by

$$\gamma_k = \begin{pmatrix} 0 & -i\sigma_k \\ i\sigma_k & 0 \end{pmatrix} \quad \gamma_4 = \begin{pmatrix} I & 0 \\ 0 & -I \end{pmatrix}. \quad (\text{B.110})$$

σ_k are 2×2 Pauli matrices. In the presence of electromagnetic couplings, the Dirac equation becomes

$$\left(\frac{\partial}{\partial x_\mu} - \frac{ie}{\hbar c} A_\mu \right) \gamma_\mu \psi + \frac{mc}{\hbar} \psi = 0, \quad (\text{B.111})$$

and the time dependence of ψ is given by $\psi = \psi(\mathbf{x}, t)|_{t=0} e^{-iEt/\hbar}$. Then we can write the coupled equations

$$\left[\boldsymbol{\sigma} \cdot \left(\mathbf{p} - \frac{e\mathbf{A}}{c} \right) \right] \psi_B = \frac{1}{c} (E - eA_0 - mc^2) \psi_A, \quad (\text{B.112})$$

$$- \left[\boldsymbol{\sigma} \cdot \left(\mathbf{p} - \frac{e\mathbf{A}}{c} \right) \right] \psi_A = -\frac{1}{c} (E - eA_0 + mc^2) \psi_B, \quad (\text{B.113})$$

with $A_\mu = (\mathbf{A}, iA_0)$. The wave function of the stationary states in the standard representation is

$$\psi = \begin{pmatrix} \psi_A \\ \psi_B \end{pmatrix} = \begin{pmatrix} g(r) \mathcal{Y}_{j l_A}^{j_3} \\ i f(r) \mathcal{Y}_{j l_B}^{j_3} \end{pmatrix} \quad (\text{B.114})$$

where $\mathcal{Y}_{j l}^{j_3}$ is normalized spin-angular function which is formed by the combination of Pauli spinor with spherical harmonics of order l . The spin-angular functions in two-component form is

$$\mathcal{Y}_{j=l\pm\frac{1}{2}, l}^{j_3} = \pm \sqrt{\frac{l \pm j_3 + \frac{1}{2}}{2l+1}} Y_l^{j_3 - \frac{1}{2}} \begin{pmatrix} 1 \\ 0 \end{pmatrix} + \sqrt{\frac{l \mp j_3 + \frac{1}{2}}{2l+1}} Y_l^{j_3 + \frac{1}{2}} \begin{pmatrix} 0 \\ 1 \end{pmatrix} \quad (\text{B.115})$$

The radial function f and g depends on k . The Dirac equation transform into the following form with scalar potential only

$$c(\boldsymbol{\sigma} \cdot \mathbf{p}) \psi_B = (E - V(r) - mc^2) \psi_A, \quad (\text{B.116})$$

$$c(\boldsymbol{\sigma} \cdot \mathbf{p}) \psi_A = (E - V(r) + mc^2) \psi_B. \quad (\text{B.117})$$

Using the identity $(\boldsymbol{\sigma}\cdot\mathbf{a})(\boldsymbol{\sigma}\cdot\mathbf{b}) = \mathbf{a}\cdot\mathbf{b} + i\boldsymbol{\sigma}\cdot(\mathbf{a}\times\mathbf{b})$, we can write $\boldsymbol{\sigma}\cdot\mathbf{p}$

$$\begin{aligned}\boldsymbol{\sigma}\cdot\mathbf{p} &= \frac{(\boldsymbol{\sigma}\cdot\mathbf{x})}{r^2}(\boldsymbol{\sigma}\cdot\mathbf{x})(\boldsymbol{\sigma}\cdot\mathbf{p}) \\ &= \frac{(\boldsymbol{\sigma}\cdot\mathbf{x})}{r^2} \left(-i\hbar r \frac{\partial}{\partial r} + i\boldsymbol{\sigma}\cdot\mathbf{L} \right).\end{aligned}\quad (\text{B.118})$$

Operator $\frac{\boldsymbol{\sigma}\cdot\mathbf{x}}{r}$ acting on $\mathcal{Y}_{jl}^{j_3}$ will give an eigenfunction of \mathbf{J}^2 , J_3 , and \mathbf{L}^2 with the same j and j_3 but of opposite orbital parity, which means

$$\frac{(\boldsymbol{\sigma}\cdot\mathbf{x})}{r} \mathcal{Y}_{jl_B}^{j_3} = -\mathcal{Y}_{jl_A}^{j_3}, \quad (\text{B.119})$$

and

$$\frac{(\boldsymbol{\sigma}\cdot\mathbf{x})}{r} \mathcal{Y}_{jl_A}^{j_3} = \mathcal{Y}_{jl_B}^{j_3}. \quad (\text{B.120})$$

Thus

$$\begin{aligned}(\boldsymbol{\sigma}\cdot\mathbf{p})\psi_B &= i \frac{(\boldsymbol{\sigma}\cdot\mathbf{x})}{r^2} \left(-i\hbar r \frac{\partial}{\partial r} + i\boldsymbol{\sigma}\cdot\mathbf{L} \right) f(r) \mathcal{Y}_{jl_B}^{j_3} \\ &= i \frac{(\boldsymbol{\sigma}\cdot\mathbf{x})}{r^2} \left(-i\hbar r \frac{\partial f}{\partial r} + i(k-1)\hbar f \right) \mathcal{Y}_{jl_B}^{j_3} \\ &= -\hbar \frac{df}{dr} \mathcal{Y}_{jl_A}^{j_3} - \frac{(1-k)\hbar}{r} f \mathcal{Y}_{jl_A}^{j_3}.\end{aligned}\quad (\text{B.121})$$

Similarly,

$$(\boldsymbol{\sigma}\cdot\mathbf{p})\psi_A = i\hbar \frac{dg}{dr} \mathcal{Y}_{jl_B}^{j_3} + i \frac{(1+k)\hbar}{r} g \mathcal{Y}_{jl_B}^{j_3}. \quad (\text{B.122})$$

We can rewrite the equations Eq. (B.116) and Eq. (B.117), using Eq. (B.121) and Eq. (B.122)

$$-c\hbar \frac{df}{dr} - \frac{(1-k)\hbar}{r} f = (E - V - mc^2)g, \quad (\text{B.123})$$

$$c\hbar \frac{dg}{dr} + \frac{(1+k)\hbar}{r} g = (E - V + mc^2)f. \quad (\text{B.124})$$

Introducing new parameter

$$F(r) = rf(r), \quad G(r) = rg(r), \quad (\text{B.125})$$

we get radial equations

$$\hbar c \left(\frac{dF}{dr} - \frac{k}{r} F \right) = -(E - V - mc^2)G, \quad (\text{B.126})$$

$$\hbar c \left(\frac{dG}{dr} + \frac{k}{r} G \right) = (E - V + mc^2)F. \quad (\text{B.127})$$

For hydrogen atom the scalar potential V is given by

$$V = -\frac{Ze^2}{4\pi r}. \quad (\text{B.128})$$

To make equations Eq. (B.126) and Eq. (B.127) more convenient, introducing more parameters

$$\alpha_1 = \frac{(mc^2 + E)}{\hbar c}, \quad \alpha_2 = \frac{(mc^2 - E)}{\hbar c}, \quad (\text{B.129})$$

$$\gamma = \frac{Ze^2}{4\pi\hbar c} = Z\alpha \equiv \frac{Z}{137}, \quad \rho = \sqrt{\alpha_1\alpha_2}r, \quad (\text{B.130})$$

and which changes the coupled equations as follows

$$\left(\frac{d}{d\rho} - \frac{k}{\rho} \right) F - \left(\sqrt{\frac{\alpha_2}{\alpha_1}} - \frac{\gamma}{\rho} \right) G = 0, \quad (\text{B.131})$$

$$\left(\frac{d}{d\rho} + \frac{k}{\rho} \right) G - \left(\sqrt{\frac{\alpha_1}{\alpha_2}} + \frac{\gamma}{\rho} \right) F = 0. \quad (\text{B.132})$$

Similar to the non relativistic treatment of the hydrogen atom, the solutions to Eq. (B.131) and Eq. (B.132) is of the form

$$F = e^{-\rho} \rho^s \sum_{m=0} a_m \rho^m, \quad G = e^{-\rho} \rho^s \sum_{m=0} b_m \rho^m. \quad (\text{B.133})$$

Substituting Eq. (B.133) in Eq. (B.131) and Eq. (B.132), and equating the coefficients of $e^{-\rho} \rho^s \rho^{q-1}$, we get the recursion relations

$$(s + q - k)a_q - a_{q-1} + \gamma b_q - \sqrt{\frac{\alpha_2}{\alpha_1}} b_{q-1} = 0, \quad (\text{B.134})$$

$$(s + q + k)b_q - b_{q-1} - \gamma a_q - \sqrt{\frac{\alpha_1}{\alpha_2}} a_{q-1} = 0. \quad (\text{B.135})$$

For $q = 0$, we have

$$(s - k)a_0 + \gamma b_0 = 0, \quad (s + k)b_0 - \gamma a_0 = 0. \quad (\text{B.136})$$

Here a_0 and b_0 are not zero, the secular determinant of Eq. (B.136) must vanish; hence

$$s = \pm \sqrt{k^2 - \gamma^2}. \quad (\text{B.137})$$

To keep $\int \psi^\dagger \psi d^3x$ finite, the condition to be fulfilled is

$$\int |F|^2 d\rho < \infty, \quad \int |G|^2 d\rho < \infty. \quad (\text{B.138})$$

Thus F and G must not diverge at the origin, $s > -\frac{1}{2}$. To fulfill

$$k^2 - \gamma^2 \geq \min(k^2) - \gamma^2 \simeq 1 - \left(\frac{Z}{137}\right)^2, \quad (\text{B.139})$$

the above requirement, we need to take the positive root of Eq. (B.137).

F and G would increase exponentially as $\rho \rightarrow \infty$ if the power series did not terminate. Assuming that the two power series terminate with the same power, n_r , where,

$$a_{n_r+1} = b_{n_r+1} = 0, \quad a_{n_r} \neq 0, b_{n_r} \neq 0. \quad (\text{B.140})$$

Setting $q = n_r + 1$ in Eq. (B.134) and Eq. (B.135), we obtain,

$$a_{n_r} = -\sqrt{\frac{\alpha_2}{\alpha_1}} b_{n_r}. \quad (\text{B.141})$$

Now setting $q = n_r$, multiplying Eq. (B.134) by α_1 , Eq. (B.135) by $\sqrt{\alpha_1 \alpha_2}$, and subtracting

$$[\alpha_1(s + n_r - k) + \gamma\sqrt{\alpha_1 \alpha_2}] a_{n_r} - [\sqrt{\alpha_1 \alpha_2}(s + n_r + k) - \gamma\alpha_1] b_{n_r} = 0. \quad (\text{B.142})$$

Using Eq. (B.141) in Eq. (B.142)

$$-\sqrt{\alpha_1 \alpha_2}(s + n_r - k) - \gamma\alpha_2 - \sqrt{\alpha_1 \alpha_2}(s + n_r + k) + \gamma\alpha_1 = 0 \quad (\text{B.143})$$

$$2\sqrt{\alpha_1 \alpha_2}(s + n_r) = \gamma(\alpha_1 - \alpha_2). \quad (\text{B.144})$$

After putting the values of α_1 and α_2 , we have

$$\sqrt{(mc^2)^2 - E^2}(s + n_r) = E\gamma. \quad (\text{B.145})$$

Squaring this, gives

$$((mc^2)^2 - E^2)(s + n_r)^2 = E^2\gamma^2 \quad (\text{B.146})$$

$$E^2((s + n_r)^2 + \gamma^2) = (mc^2)^2(s + n_r)^2$$

$$E^2 = \frac{(mc^2)^2(s + n_r)^2}{(s + n_r)^2 + \gamma^2}$$

$$E^2 = \frac{(mc^2)^2}{1 + \left(\frac{\gamma}{s+n_r}\right)^2}$$

$$E = \frac{mc^2}{\sqrt{1 + \left(\frac{\gamma}{s+n_r}\right)^2}}$$

$$= \frac{mc^2}{\sqrt{1 + \frac{Z^2\alpha^2}{\left(n_r + \sqrt{(j+\frac{1}{2})^2 - Z^2\alpha^2}\right)^2}}}. \quad (\text{B.147})$$

Expanding Eq. (B.147) gives

$$E = mc^2 \left[1 + \frac{Z^2\alpha^2}{\left(n_r + \sqrt{(j+\frac{1}{2})^2 - Z^2\alpha^2}\right)^2} \right]^{-\frac{1}{2}} \quad (\text{B.148})$$

$$= mc^2 \left[1 - \frac{1}{2} \frac{(Z\alpha)^2}{n^2} - \frac{1}{2} \frac{(Z\alpha)^4}{n^3} \left(\frac{1}{j+\frac{1}{2}} - \frac{3}{4n} \right) - \dots \right]. \quad (\text{B.149})$$

For the ground state, $n_r = 0$, $k = -1$ (spin parallel to angular momentum), Eq. (B.147) becomes

$$\begin{aligned} E_{gd} &= mc^2 \frac{1}{\sqrt{1 + \frac{Z^2\alpha^2}{(j+\frac{1}{2})^2 - Z^2\alpha^2}}} \\ &= mc^2 \frac{1}{\sqrt{\frac{(j+\frac{1}{2})^2 - Z^2\alpha^2 + Z^2\alpha^2}{(j+\frac{1}{2})^2 - Z^2\alpha^2}}} \\ &= mc^2 \sqrt{\frac{(j+\frac{1}{2})^2 - Z^2\alpha^2}{(j+\frac{1}{2})^2}} \\ &= mc^2 \sqrt{1 - Z^2\alpha^2}. \end{aligned} \quad (\text{B.150})$$

Using Eq. (B.150),

$$\begin{aligned}
\sqrt{\alpha_1 \alpha_2} &= \frac{1}{\hbar c} \sqrt{(mc^2)^2 - (mc^2)^2(1 - Z^2 \alpha^2)} \\
&= \frac{1}{\hbar c} mc^2 Z \alpha \\
&= \frac{Z}{a_B},
\end{aligned} \tag{B.151}$$

where $a_B = \frac{\hbar}{\alpha mc}$. Using Eq. (B.141)

$$\begin{aligned}
a_0 &= -\sqrt{\frac{\alpha_2}{\alpha_1}} b_0 \\
&= -\frac{\sqrt{\alpha_1 \alpha_2}}{\alpha_1} b_0 \\
&= -\frac{\frac{Z \alpha mc^2}{\hbar c}}{\frac{mc^2 + E}{\hbar c}} b_0 \\
&= -\frac{Z \alpha mc^2}{mc^2 + mc^2 \sqrt{1 - (Z \alpha)^2}} b_0 \\
\frac{a_0}{b_0} &= -\frac{Z \alpha}{1 + \sqrt{1 - (Z \alpha)^2}}.
\end{aligned} \tag{B.152}$$

Let us find the wave function, using Eq. (B.125) in Eq. (B.114), we can write

$$\begin{aligned}
\psi &= \begin{pmatrix} \psi_A \\ \psi_B \end{pmatrix} = \begin{pmatrix} g(r) \mathcal{Y}_{j l_A}^{j_3} \\ i f(r) \mathcal{Y}_{j l_B}^{j_3} \end{pmatrix} \\
&= \begin{pmatrix} \frac{G(r)}{r} \mathcal{Y}_{j l_A}^{j_3} \\ \frac{F(r)}{r} \mathcal{Y}_{j l_B}^{j_3} \end{pmatrix}.
\end{aligned} \tag{B.153}$$

For ground state wave function, $n_r = 0$ and $k = -1$

$$s = \sqrt{1 - (Z \alpha)^2}, \quad \rho = \frac{Z r}{a_B}. \tag{B.154}$$

Inserting $m = n_r = 0$ in Eq. (B.133)

$$\begin{aligned}
F &= e^{-\rho} \rho^s \sum_{m=0} a_m \rho^m, & G &= e^{-\rho} \rho^s \sum_{m=0} b_m \rho^m \\
&= e^{-\frac{Z r}{a_B}} \left(\frac{Z r}{a_B} \right)^{\sqrt{1 - (Z \alpha)^2}} a_0, & &= e^{-\frac{Z r}{a_B}} \left(\frac{Z r}{a_B} \right)^{\sqrt{1 - (Z \alpha)^2}} b_0.
\end{aligned} \tag{B.155}$$

Using Eq. (B.155) in Eq. (B.153), the wave function becomes

$$\begin{aligned}
\psi &= N \begin{pmatrix} e^{-\frac{Zr}{a_B}} \left(\frac{Zr}{a_B}\right)^{\sqrt{1-(Z\alpha)^2}} \frac{1}{r} b_0 \mathcal{Y}_{j l_A}^{j_3} \\ i e^{-\frac{Zr}{a_B}} \left(\frac{Zr}{a_B}\right)^{\sqrt{1-(Z\alpha)^2}} \frac{1}{r} a_0 \mathcal{Y}_{j l_B}^{j_3} \end{pmatrix} \\
&= N e^{-\frac{Zr}{a_B}} \left(\frac{Z}{a_B}\right) \left(\frac{Zr}{a_B}\right)^{\sqrt{1-(Z\alpha)^2}-1} \begin{pmatrix} b_0 \mathcal{Y}_{j l_A}^{j_3} \\ i a_0 \frac{\boldsymbol{\sigma} \cdot \mathbf{x}}{r} \mathcal{Y}_{j l_A}^{j_3} \end{pmatrix} \\
&= N e^{-\frac{Zr}{a_B}} \left(\frac{Z}{a_B}\right) \left(\frac{Zr}{a_B}\right)^{\sqrt{1-(Z\alpha)^2}-1} \begin{pmatrix} b_0 \mathcal{Y}_{j l_A}^{j_3} \\ -i \frac{Z\alpha}{1+\sqrt{1-(Z\alpha)^2}} b_0 \frac{\boldsymbol{\sigma} \cdot \mathbf{x}}{r} \mathcal{Y}_{j l_A}^{j_3} \end{pmatrix} \\
&= N b_0 e^{-\frac{Zr}{a_B}} \left(\frac{Z}{a_B}\right) \left(\frac{Zr}{a_B}\right)^{\sqrt{1-(Z\alpha)^2}-1} \begin{pmatrix} Y_0^0 \chi^s \\ -i \frac{Z\alpha}{1+\sqrt{1-(Z\alpha)^2}} \frac{\boldsymbol{\sigma} \cdot \mathbf{x}}{r} (-Y_0^0 \chi^s) \end{pmatrix} \\
&= \frac{N b_0}{2\sqrt{\pi}} e^{-\frac{Zr}{a_B}} \left(\frac{Z}{a_B}\right) \left(\frac{Zr}{a_B}\right)^{\sqrt{1-(Z\alpha)^2}-1} \begin{pmatrix} \chi^s \\ i \left(\frac{1-\sqrt{1-(Z\alpha)^2}}{Z\alpha}\right) \frac{\boldsymbol{\sigma} \cdot \mathbf{x}}{r} \chi^s \end{pmatrix}. \tag{B.156}
\end{aligned}$$

Introducing new constant and parameter,

$$\tilde{N} = \frac{N b_0}{2\sqrt{\pi}} \left(\frac{Z}{a_B}\right), \quad \mu = \sqrt{1-(Z\alpha)^2}, \tag{B.157}$$

in Eq. (B.156)

$$\psi = \tilde{N} e^{-\frac{Zr}{a_B}} \left(\frac{Zr}{a_B}\right)^{\mu-1} \begin{pmatrix} \chi^s \\ i \frac{1-\mu}{Z\alpha} \frac{\boldsymbol{\sigma} \cdot \mathbf{x}}{r} \chi^s \end{pmatrix}, \tag{B.158}$$

where \tilde{N} is the normalization constant. To find the normalization constant, have to calculate

the integration

$$\int_{-\infty}^{\infty} \psi^* \psi dV = 1 \quad (\text{B.159})$$

$$\int_{-\infty}^{\infty} \tilde{N}^2 e^{-\frac{2Zr}{a_B}} \left(\frac{Zr}{a_B}\right)^{2[\mu-1]} \left(\chi^{s^*} \chi^s + \frac{(1-\mu)^2}{Z^2 \alpha^2} \chi^{s^*} \chi^s\right) r^2 \sin \theta d\theta d\phi dr = 1 \quad (\text{B.160})$$

$$\frac{4\pi}{2^{2(\mu-1)}} \left(1 + \frac{(1-\mu)^2}{Z^2 \alpha^2}\right) \tilde{N}^2 \int_{-\infty}^{\infty} e^{-\frac{2Zr}{a_B}} \left(\frac{2Zr}{a_B}\right)^{2(\mu-1)} r^2 dr = 1 \quad (\text{B.161})$$

$$\frac{4\pi}{\left(\frac{2Z}{a_B}\right)^2 2^{2(\mu-1)}} \left(1 + \frac{(1-\mu)^2}{Z^2 \alpha^2}\right) \tilde{N}^2 \int_{-\infty}^{\infty} e^{-\frac{2Zr}{a_B}} \left(\frac{2Zr}{a_B}\right)^{2\mu} dr = 1 \quad (\text{B.162})$$

$$\frac{2 \times 4\pi}{\left(\frac{2Z}{a_B}\right)^2 2^{2(\mu-1)} \frac{2Z}{a_B}} \left(1 + \frac{(1-\mu)^2}{Z^2 \alpha^2}\right) \tilde{N}^2 \int_0^{\infty} e^{-\frac{2Zr}{a_B}} \left(\frac{2Zr}{a_B}\right)^{2\mu} d\left(\frac{2Zr}{a_B}\right) = 1 \quad (\text{B.163})$$

$$\frac{4\pi}{\left(\frac{Z}{a_B}\right)^3 2^{2\mu}} \left(1 + \frac{(1-\mu)^2}{Z^2 \alpha^2}\right) \tilde{N}^2 \Gamma(1 + 2\mu) = 1, \quad (\text{B.164})$$

using the integral

$$\Gamma(1 + x) = \int_0^{\infty} e^{-t} t^x dt. \quad (\text{B.165})$$

Finally the normalization constant becomes

$$\tilde{N}^2 = \frac{\left(\frac{Z}{a_B}\right)^3 2^{2\mu-2}}{\pi \left(1 + \frac{(1-\mu)^2}{Z^2 \alpha^2}\right) \Gamma(1 + 2\mu)} \quad (\text{B.166})$$

$$\tilde{N} = 2^{\mu-1} \left(\frac{Z}{a_B}\right)^{3/2} \frac{1}{\sqrt{\pi}} \sqrt{\frac{1}{\left(1 + \frac{(1-\mu)^2}{Z^2 \alpha^2}\right) \Gamma(1 + 2\mu)}} \quad (\text{B.167})$$

$$= 2^{\sqrt{1-(Z\alpha)^2}-1} \left(\frac{Z}{a_B}\right)^{3/2} \frac{1}{\sqrt{\pi}} \sqrt{\frac{1}{\left(1 + \frac{(1-\sqrt{1-(Z\alpha)^2})^2}{Z^2 \alpha^2}\right) \Gamma\left(1 + 2\sqrt{1-(Z\alpha)^2}\right)}} \quad (\text{B.168})$$

$$= 2^{\sqrt{1-(Z\alpha)^2}-1} \left(\frac{Z}{a_B}\right)^{3/2} \frac{1}{\sqrt{\pi}} \sqrt{\frac{1 + \sqrt{1-(Z\alpha)^2}}{2\Gamma\left(1 + 2\sqrt{1-(Z\alpha)^2}\right)}}. \quad (\text{B.169})$$

The wave function with the normalization constant

$$\begin{aligned} \psi = & 2\sqrt{1-(Z\alpha)^2-1} \left(\frac{Z}{a_B}\right)^{3/2} \frac{1}{\sqrt{2}\sqrt{\pi}} \sqrt{\frac{1+\sqrt{1-(Z\alpha)^2}}{\Gamma(1+2\sqrt{1-(Z\alpha)^2})}} e^{-\frac{Zr}{a_B}} \left(\frac{Zr}{a_B}\right)^{\sqrt{1-(Z\alpha)^2-1}} \\ & \times \left(i \frac{\chi^s}{Z\alpha} \frac{1-\sqrt{1-(Z\alpha)^2}}{r} \frac{\boldsymbol{\sigma}\cdot\mathbf{x}}{r} \chi^s \right). \end{aligned} \quad (\text{B.170})$$